Available online at www.sciencedirect.com
ScienceDirect
Journal of Volcanology and Geothermal Research 161 (2007) 187–214
Journal of volcanology and geothermal research
www.elsevier.com/locate/jvolgeores

Distribution and geochronology of Oregon Plateau (U.S.A.) flood basalt volcanism: The Steens Basalt revisited

Matthew E. Brueseke [a,*], Matthew T. Heizler [b], William K. Hart [c], Stanley A. Mertzman [d]

[a] Department of Geology/Geography, Eastern Illinois University, 600 Lincoln Avenue Charleston, IL 61920, United States
[b] New Mexico Bureau of Geology and Mineral Resources, New Mexico Tech, 801 Leroy Place, Socorro, NM 87801, United States
[c] Department of Geology, Miami University, 114 Shideler Hall, Oxford, OH 45056, United States
[d] Department of Earth and Environment, Franklin and Marshall College, P.O. Box 3003, Lancaster, PA 17604, United States

Received 28 July 2005; received in revised form 18 December 2006; accepted 19 December 2006
Available online 8 January 2007

Abstract

The timing and petrogenesis of mid-Miocene flood basalt volcanism in the northwest United States has been extensively addressed, yet the chemical characteristics and temporal details of the Steens Basalt, exposed on the Oregon Plateau, are poorly defined. Steens Basalt volcanism has generally been accepted to have occurred at ~16.6 Ma, coeval and/or just prior to the onset of Columbia River Basalt Group volcanism to the north. New major and trace element analyses and nine $^{40}Ar/^{39}Ar$ ages ranging from 15.51±0.28 to 16.58±0.18 Ma were obtained on Oregon Plateau flood basalt lava flows from stratigraphic sections in close proximity to Steens Mountain. Additionally, new $^{40}Ar/^{39}Ar$ ages were obtained on the uppermost and thirty-first lava flow down from the top of the ~1 km section of Steens Basalt exposed at Steens Mountain and yield eruption ages of 16.59±0.10 and 16.55±0.10 Ma, respectively. Field relations between these basalt sections suggest that multiple eruptive centers were present in the vicinity of Steens Mountain.

The chemical and chronologic data presented in this study illustrate that flood basalts with the "Steens Basalt" chemical signature erupted across the southern Oregon Plateau over a much greater timespan than what is typically quoted for the Steens Mountain type section. These data suggest that the main volume of Steens Basalt volcanism erupted over at least an ~1 m.y. duration from eruptive loci in the vicinity of Steens Mountain, while likely much less voluminous volcanism and lithospheric input of mafic magma appears to have occurred for >2 Ma across the Oregon Plateau. These new geochemical and geochronological constraints verify a common temporal link between Steens, Malheur Gorge-region, and Columbia River Basalt Group (CRBG) volcanism. This direct temporal link requires that petrogenetic and tectonic models of mid-Miocene northwestern U.S. flood basalt volcanism recognize that the northern (Columbia Plateau) and southern (Oregon Plateau) portions of this mid-Miocene basalt province were erupting simultaneously during portions of the regional event.

Keywords: Steens Mountain; Oregon Plateau; Miocene; flood basalts; $^{40}Ar/^{39}Ar$; Yellowstone

1. Introduction and regional geology

Large volumes of dominantly tholeiitic basalts and ferroandesites started erupting at ~17 Ma in the Pacific Northwest of the United States from loci juxtaposed against the western margin of the Wyoming Craton.

* Corresponding author. Tel.: +1 217 581 2827; fax: +1 217 581 6613.
E-mail address: mebrueseke@eiu.edu (M.E. Brueseke).

0377-0273/$ - see front matter © 2007 Elsevier B.V. All rights reserved.
doi:10.1016/j.jvolgeores.2006.12.004

These eruptions occurred during a cessation in regional subduction- and extension-related calc-alkaline volcanism (Carlson and Hart, 1987; Hooper, 2000; John, 2001). This mid-Miocene magmatic event is dominated by the Columbia River Basalt Group (CRBG) and Oregon Plateau mafic lava flows, both of which are the manifestations of the Yellowstone/Newberry melting anomaly (hotspot) and/or regional tectonic interaction between the underlying mantle and reactivated lithospheric structures (Christiansen and McKee, 1978; Carlson and Hart, 1987; Zoback et al., 1994; Dickinson, 1997; Humphreys et al., 2000; John and Wallace, 2000; Wagner et al., 2000; Christiansen et al., 2002; Glen and Ponce, 2002; Jordan et al., 2004; Camp and Ross, 2004). The CRBG is widely recognized as one of Earth's modern flood basalt provinces, and following the definitions and descriptions of other flood basalt provinces provided by Walker (1993), we consider the temporally similar and volumetrically substantial Oregon Plateau mafic lava package to define a flood basalt sequence.

The stratigraphic and chronologic details of CRBG flood basalt volcanism are fairly well constrained (Tolan et al., 1989; Baksi and Farrar, 1990), whereas the stratigraphic details and temporal relationships of Oregon Plateau flood basalt volcanism (cf. Steens Basalt) are less well understood. Additionally, unlike the eruptive products of the CRBG, it is often asserted that the Steens Basalt erupted in one brief magmatic event at ~16.6 Ma (Swisher et al., 1990; Hooper, 1997; Johnson et al., 1998; Hooper et al., 2002; Camp et al., 2003; Camp and Ross, 2004), contemporaneous with and/or preceding the earliest Imnaha Basalt of the CRBG. The thickest exposures of Oregon Plateau mafic volcanism tend to be found in the vicinity of Steens Mountain (Steens Basalt sensu-stricto), however, eruptive loci (dikes) and eruptive products are present across the southern Oregon Plateau and its margins (Larson et al., 1971; Hart and Carlson, 1985; Mankinen et al., 1987; Brueseke et al., 2003; Brueseke and Hart, 2004; Colgan et al., 2006; Brueseke and Hart, in press) (Fig. 1a and b). Some workers have interpreted these data to indicate that Steens Basalt volcanism was initially widespread across the Oregon Plateau, and gradually shifted to one large eruptive center situated at Steens Mountain (Mankinen et al., 1987). Accompanying this spatial shift, one large magmatic event then occurred centered at Steens Mountain, forming the upper part of the ~75 to 100 flow, ~900 to 1000 m thick section of Steens Basalt, with outflow found as far west as Abert and Poker Jim Rims, Oregon and as far south as northern Nevada (Hart and Mertzman, 1982; Carlson and Hart, 1983; Hart and Carlson, 1985; Mankinen et al., 1987). Earlier paleomagnetic results on the Steens Basalt type section documented a N/R (normal polarity over reversed) paleomagnetic reversal within the upper portion of the flood basalt section and this reversal, the presence of thin lava flows, and the lack of thick interflow sedimentary horizons, were taken to indicate that the entire sequence of lava flows was erupted over a very short period of time (2000–50,000 yr; Baksi et al., 1967; Gunn and Watkins, 1970; Grommé et al., 1985; Mankinen et al., 1985; Mankinen et al., 1987).

Prior $^{40}Ar/^{39}Ar$ geochronology yield indistinguishable ~16.6 Ma chronologic results for the uppermost and 31st (down from the top) flows of the Steens Basalt type section (Swisher et al., 1990), and additional $^{40}Ar/^{39}Ar$ ages from below these stratigraphic levels yield similar ages (Baksi and Farrar, 1990; Baksi et al., 1991). The data and interpretations of Hart and Mertzman (1982), Carlson and Hart (1983), Hart and Carlson (1985), and Carlson and Hart (1987) left open the possibility that the type Steens Basalt section might not

Fig. 1. (a) Map of the northwestern United States depicting select Cenozoic volcanic and tectonic features. Shaded region is the approximate extent of mid-Miocene flood basalt volcanism (after Hart and Carlson, 1985; Camp and Ross, 2004). Also shown are major flood basalt dike swarms/eruptive loci (black lines), Malheur Gorge-region (MG), Oregon–Idaho graben (OIG) and Northern Nevada rift (NNR) and associated magnetic anomalies corresponding to zones of lithospheric extension/mafic magma emplacement (black dashed lines; Cummings et al., 2000; Glen and Ponce, 2002), commonly depicted volcanic fields of the Yellowstone–Snake River plain province (dashed circles); BJ, Bruneau–Jarbidge (~12.5 to <11 Ma); TF, Twin Falls (~10 to 8.6 Ma); PC, Picabo (~10 Ma); HS, Heise (~6.7 to 4.3 Ma); and YS, Yellowstone (<2.5 Ma), and age isochrons (dashed lines, ages in Ma) of Oregon High Lava Plains silicic volcanism (N, Newberry Volcano; after Jordan et al., 2004). These two trends originate in the Oregon Plateau, which was characterized by abundant silicic volcanic loci and volcanic fields during the mid-Miocene (e.g. McDermitt, Santa Rosa–Calico). Also illustrated are the initial $^{87}Sr/^{86}Sr$ 0.706 and 0.704 isopleths (after Armstrong et al., 1977; Kistler and Peterman, 1978; Leeman et al., 1992; Crafford and Grauch, 2002), which are commonly interpreted to demarcate the western edge of the Precambrian North American craton (the 0.706 isopleth) and a zone of transitional lithosphere between the older craton and Mesozoic accreted terranes to the west (between the 0.706 and 0.704 isopleth). (b) Shaded digital elevation model of the southeastern Oregon Plateau depicting documented flood basalt eruptive loci, study area (dashed box) and sampled section locations, and regional geographic and tectonic features. White circles indicate southeastern Oregon Plateau flood basalt eruptive loci/shallow intrusive bodies. Notice widespread location of Steens Basalt eruptive loci and lack of loci identified/exposed on the Owyhee Plateau portion of the Oregon Plateau. SM, Steens Mountain fault scarp and its southern continuation, the Pueblo Mountains; OIG, Oregon–Idaho graben; OM, Owyhee mountains; WSRP, western Snake River Plain; OWP, Owyhee Plateau; BR-T, Bull Run–Tuscarora Mountains; NNR, eastern northern Nevada rift; SC, Santa Rosa–Calico volcanic field; MD, McDermitt volcanic field.

be representative of the entire Steens Basalt, and hence Oregon Plateau flood basalt magmatic event. Regardless, subsequent workers have typically quoted the ~16.6 Ma type section age as solely representative of the entire duration of Steens Basalt volcanism. In this study we demonstrate that Oregon Plateau flood basalt eruptive activity was more complex than is commonly recognized and that the temporal characteristics of Oregon Plateau flood basalt volcanism are similar to other mid-Miocene Pacific Northwest flood basalt eruptions. Additionally, this study is the first detailed geochemical and geochronological examination of mid-Miocene Oregon Plateau basaltic volcanism and provides a model for future chemo- and chronostratigraphic studies of lava flow packages and flood basalt provinces.

Renewed interest has recently highlighted some of the stratigraphic and chronologic issues associated with the onset and duration of mid-Miocene flood basalt volcanism in the northwest United States (Hooper et al., 2002; Camp et al., 2003; Camp and Ross, 2004). Newly suggested stratigraphic relationships within eastern

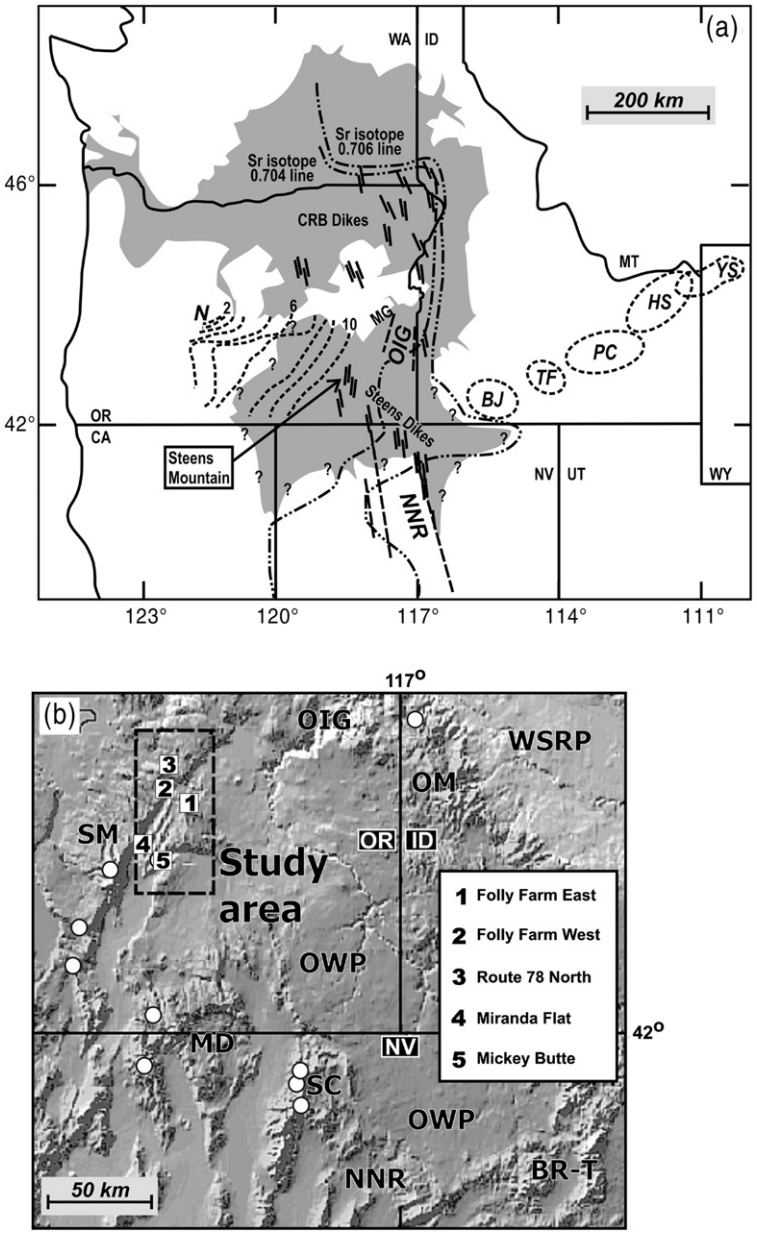

Oregon Plateau flood basalts have helped tentatively correlate lava flows erupted in the vicinity of Steens Mountain with tholeiitic volcanism further north. However, this link and its relationship with lava flows erupted throughout the entire areal extent of the Oregon Plateau are still somewhat poorly constrained. Here, we (1) present new geochemical data and $^{40}Ar/^{39}Ar$ ages obtained on mafic lava flows from the southern Oregon Plateau, including two previously dated samples from the Steens Basalt type section, (2) normalize published Oregon Plateau flood basalt and Steens Basalt ages to a common $^{40}Ar/^{39}Ar$ fluence monitor age (i.e. standard) to obtain an internally consistent eruption age for at least the upper 450 m of the Steens Mountain type section and to facilitate regional interpretations, and (3) reconsider the areal extent, duration, and regional implications of flood basalt volcanism on the Oregon Plateau. These new data document at least an ~1 m.y. duration of flood basalt volcanism in close proximity to Steens Mountain. Furthermore, major and trace element geochemistry and petrography link regionally exposed Oregon Plateau lava flows with at least the upper package of Steens Basalt exposed at Steens Mountain. Collectively, the lava flows in question are generally relatively thin and are characterized by a lack of interflow sediments, aphyric to coarsely plagioclase phyric textures, and mid-Miocene eruptive ages. These lava flows were originally studied by Fuller (1930, 1931) and later defined by Baksi et al. (1967) and Gunn and Watkins (1970) based on the sequence exposed at Steens Mountain. They are also well exposed along the Steens Mountain fault scarp to the south in the Pueblo Mountains (i.e.. the Pueblo Mountains basalt of Avent, 1970; Hart et al., 1989). Analyzed Steens Basalt samples vary chemically from olivine tholeiite and high-alumina basalt to more evolved, and sometimes mildly alkalic, basaltic andesites, trachybasalts, and basaltic trachyandesites (Gunn and Watkins, 1970; Carlson and Hart, 1983; Hart et al., 1989; Johnson et al., 1998; Camp et al., 2003; this study).

The chemical characteristics we present and discuss support earlier observations by Hart and Mertzman (1982), Carlson and Hart (1983, 1987), Hart and Carlson (1985), and Hart et al. (1989) who suggested that exposed flood basalts in this region span a greater temporal range than what is represented by the Steens Basalt type section. While presenting these observations, Hart and Carlson (1985) and Carlson and Hart (1987) divided southern Oregon Plateau ~17 to ~14 Ma flood basalt lava flows into two types: (1) mafic lava flows that are temporally, chemically, and isotopically similar to the Steens Basalt at Steens Mountain and (2) mafic lava flows with similar chemical characteristics to the Steens Basalt exposed at the type section but different temporal and isotopic characteristics. The first group was considered to be Steens Basalt that erupted from a source at Steens Mountain ca. ~16.6 Ma and primarily flowed west and south (Hart and Carlson, 1985; Carlson and Hart, 1987; Swisher et al., 1990). This group includes lava flows exposed as far west as Poker Jim and Abert Rims (OR), as far south as the Black Rock desert (NV) (Hart and Carlson, 1985; Carlson and Hart, 1987), and potentially as far east as the margin of the Santa Rosa–Calico volcanic field (NV) (Larson et al., 1971; Brueseke and Hart, in press). The second group of isotopically dissimilar lava flows, termed "Steens-Type" Basalt by Hart and Carlson (1985), includes shallow intrusive bodies, lava flows, and flow packages that are primarily exposed to the east of Steens Mountain. Stratigraphic, chronologic, chemical, and isotopic data from these lava flows indicate that they erupted between ~17 and 14 Ma (Hart and Mertzman, 1982; Hart and Carlson, 1985; Carlson and Hart, 1987). Dikes and eruptive loci of this group are well exposed in the Santa Rosa–Calico volcanic field, NV, as well as in other locations on and peripheral to the Oregon Plateau (Steens dikes and eruptive loci; Fig. 1a and b). In their study, Hart and Carlson (1985) also included much younger (~12±1 Ma), chemically and isotopically distinct tholeiitic basaltic lava flows and thin flow packages into this second, "Steens-Type" group. These younger (~12±1 Ma) basalts are characterized by slightly higher TiO_2 (2–3 wt.%), P_2O_5 (typically >0.5 wt.%), Ba (>600 ppm), and Zr (>300 ppm) concentrations than the older basalts, though they are petrographically and chemically similar in all other respects (Hart and Mertzman, 1982). Hart and Mertzman (1982) speculated that these younger basalts may be the Oregon Plateau equivalent of the <14 Ma Saddle Mountains Basalt of the Columbia River Basalt Group (CRBG); however, more work must be performed to better document their volume, areal extent, and regional significance. Based on data and interpretations that have surfaced over the past two decades, including those presented in this paper, we suggest the "Steens-Type" nomenclature be abandoned totally or at least restricted to the description of these poorly understood ~12±1 Ma lava flows. As part of this study, we demonstrate that at least some of the regional ~16±1 Ma Oregon Plateau mafic lava flows originally termed "Steens-Type" Basalt are compositionally and temporally correlative to Steens Basalt lava flows and should be considered part of the Steens Basalt eruptive sequence, even though they

erupted over a greater timespan and areal distribution than the flood basalt lava flows exposed at Steens Mountain.

2. $^{40}Ar/^{39}Ar$ methodology and age assignments

$^{40}Ar/^{39}Ar$ geochronology was conducted on eleven groundmass concentrates and one plagioclase separate at the New Mexico Geochronology Research Laboratory (NMGRL). Nine of the samples are from Oregon Plateau flood basalt lava flows collected from five stratigraphic sections within the study area, whereas two samples are from Steens Mountain. Also, one sample (MB97-2) is from an andesite lava flow exposed within a package of four compositionally similar flows that disconformably cap one of the basalt stratigraphic sections. All samples were analyzed by the furnace incremental heating age spectrum method using between nine and eleven heating steps (Table 1; Appendix A; Argon data repository). The basalts from Steens Mountain were analyzed in order to better directly compare age results from the entire study area and to determine the intercomparability of data from the NMGRL with previously published data. In addition to standard age spectrum analysis, the basalts from Steens Mountain were also analyzed by a 2-step age spectrum method that reproduces the analytical protocol used by Swisher et al. (1990). A summary of the analytical methods is presented in Table 1 and complete argon isotopic results are compiled in Appendix A. All new age data cited in the text are quoted at 2σ unless specifically noted otherwise.

Age and K/Ca spectrum diagrams along with isotopic correlation plots are given in Figs. 2 and 3 for the furnace step-heated samples. These samples yield age spectra with variable levels of complexity and methods for age assignment require some discussion. A variety of criteria for age assignment for step-heating data have circulated throughout the $^{40}Ar/^{39}Ar$ literature (cf. McDougall and Harrison, 1999). This variety is very evident when working with basaltic groundmass concentrate age spectra and adherence to strict criteria can be both beneficial and detrimental to the geochronological study. The benefits of using a pre-determined set of criteria is that it is straightforward to decide which samples yield reliable eruption ages based on the

Table 1
Summary of $^{40}Ar/^{39}Ar$ methods

Sample preparation and irradiation:
Groundmass concentrates obtained by hand-picking 1–2 mm rock fragments free of visible phenocrysts. Samples rinsed in dilute HCl followed by a thorough ultrasonic wash in distilled water. CH82 samples were picked free of coarse plagioclase, reacted with dilute HCl and HF and followed by boiling in distilled water for 1 h. Plagioclase separate hand-picked from crushed sample, washed in dilute HCl and ultrasonically cleaned in distilled water.
Samples were loaded into machined Al discs and irradiated in 3 separate packages in the D-3 position, Nuclear Science Center, College Station, TX. NM-89 and NM-110 were 7 h irradiations whereas NM-179 was 14 h.
Neutron flux monitor Fish Canyon Tuff sanidine (FC-2). Assigned age = 28.02 Ma (Renne et al., 1998).
Instrumentation:
Mass Analyzer Products 215-50 mass spectrometer on line with automated all-metal extraction system.
Most samples were step-heated in a double vacuum Mo resistance furnace.
CH82 samples also step-heated using a defocused Synrad 50 W CO_2 laser.
Flux monitor single crystal sanidines fused by a 50 W Synrad CO_2 laser.
Furnace analysis: Reactive gases removed during a 7 min heating with a SAES GP-50 getter operated at ~450 °C.
Additional cleanup (6 min) following heating with 2 SAES GP-50 getters, 1 operated at ~450 °C and 1 at 20 °C.
Gas also exposed to a W filament operated at ~2000 °C.
Laser step-heating analysis: Samples heated for 0.5–1 min.
Reactive gases removed during heating followed by a 5 min reaction with 2 SAES GP-50 getters.
1 operated at ~450 °C and 1 at 20 °C. Gas also exposed to a W filament operated at ~2000 °C and a cold finger operated at −140 °C.
Analytical parameters:
System sensitivities: NM-89 furnace = 2.3; NM-110 furnace = 3.0; NM-179 furnace = 2.88; NM-179 laser = 1.65. All values times 10^{-16} mol/pA
Total system blank and background: Furnace NM-89 = 130, 1.4, 0.1, 0.9, 0.6×10^{-17} mol for masses 40, 39, 38, 37, 36, respectively.
Total system blank and background: Furnace NM-110 = 1400, 2.6, 1.3, 0.8, 5.6×10^{-17} mol for masses 40, 39, 38, 37, 36, respectively.
Total system blank and background: Furnace NM-179 = 100, 0.7, 0.4, 0.4, 0.5×10^{-17} mol for masses 40, 39, 38, 37, 36, respectively.
Total system blank and background: Laser NM-179 = 52, 1.5, 0.1, 0.1, 0.3×10^{-17} mol for masses 40, 39, 38, 37, 36, respectively.
J-factors determined to a precision of ±0.1% (1 s) by CO_2 laser-fusion of 4–6 single crystals from each of 6–10 radial positions around the irradiation tray.
Correction factors for interfering nuclear reactions were determined using K-glass and CaF_2 and are as follows:
NM-89 and 110: $(^{40}Ar/^{39}Ar)_K = 0.0 \pm 0.0004$; $(^{36}Ar/^{37}Ar)_{Ca} = 0.000280 \pm 0.000005$; and $(^{39}Ar/^{37}Ar)_{Ca} = 0.00070 \pm 0.00002$.
NM-179: $(^{40}Ar/^{39}Ar)_K = 0.0 \pm 0.0004$; $(^{36}Ar/^{37}Ar)_{Ca} = 0.0002878 \pm 0.000003$; and $(^{39}Ar/^{37}Ar)_{Ca} = 0.0006765 \pm 0.000005$.

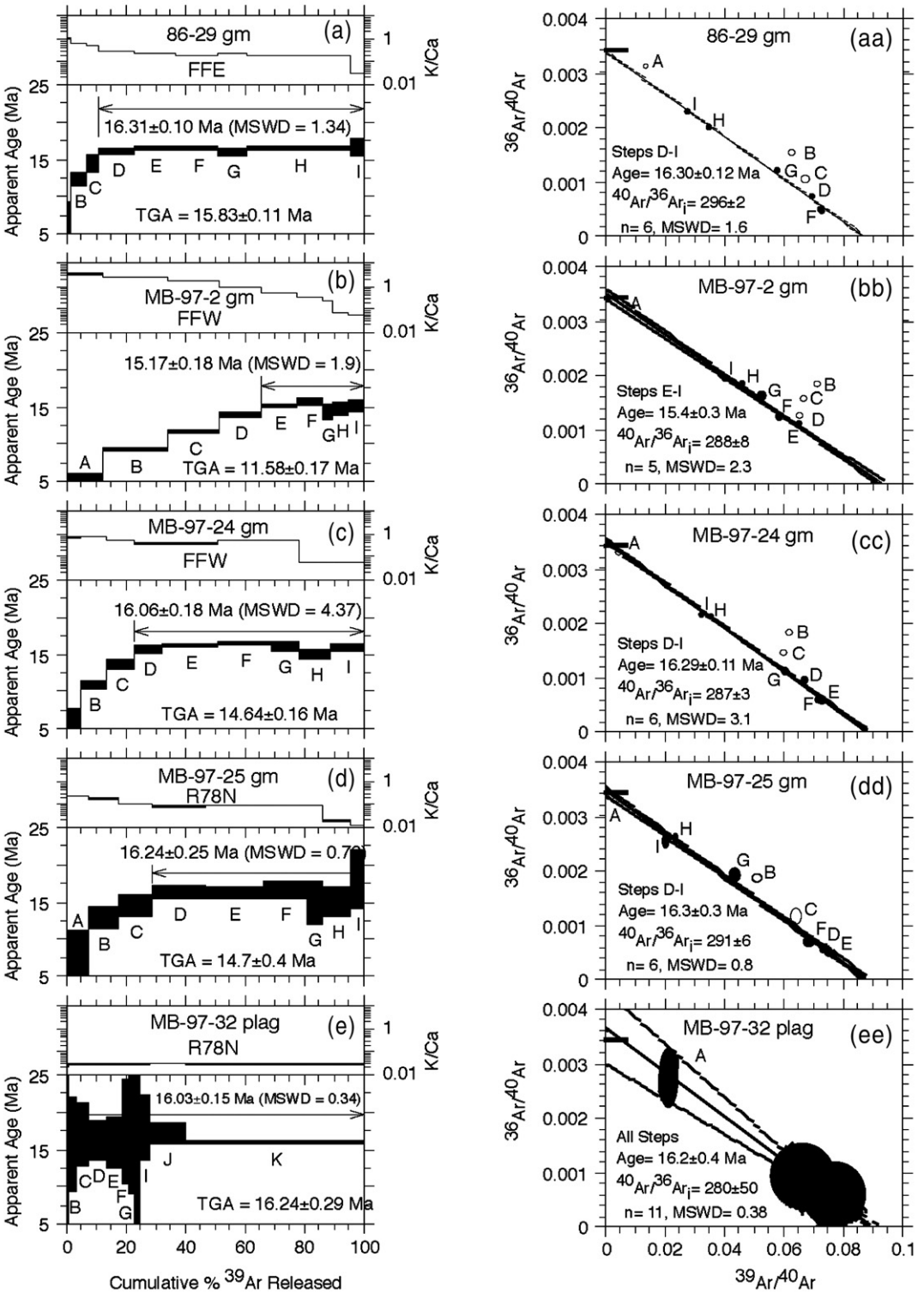

Fig. 2. a–j. $^{40}Ar/^{39}Ar$ age and K/Ca spectra for dated lava flows from stratigraphic sections peripheral to Steens Mountain. Plateau age errors are 1σ. Isotope correlation diagrams report intercept results determined by York (1969) linear regression results and errors are 1σ.

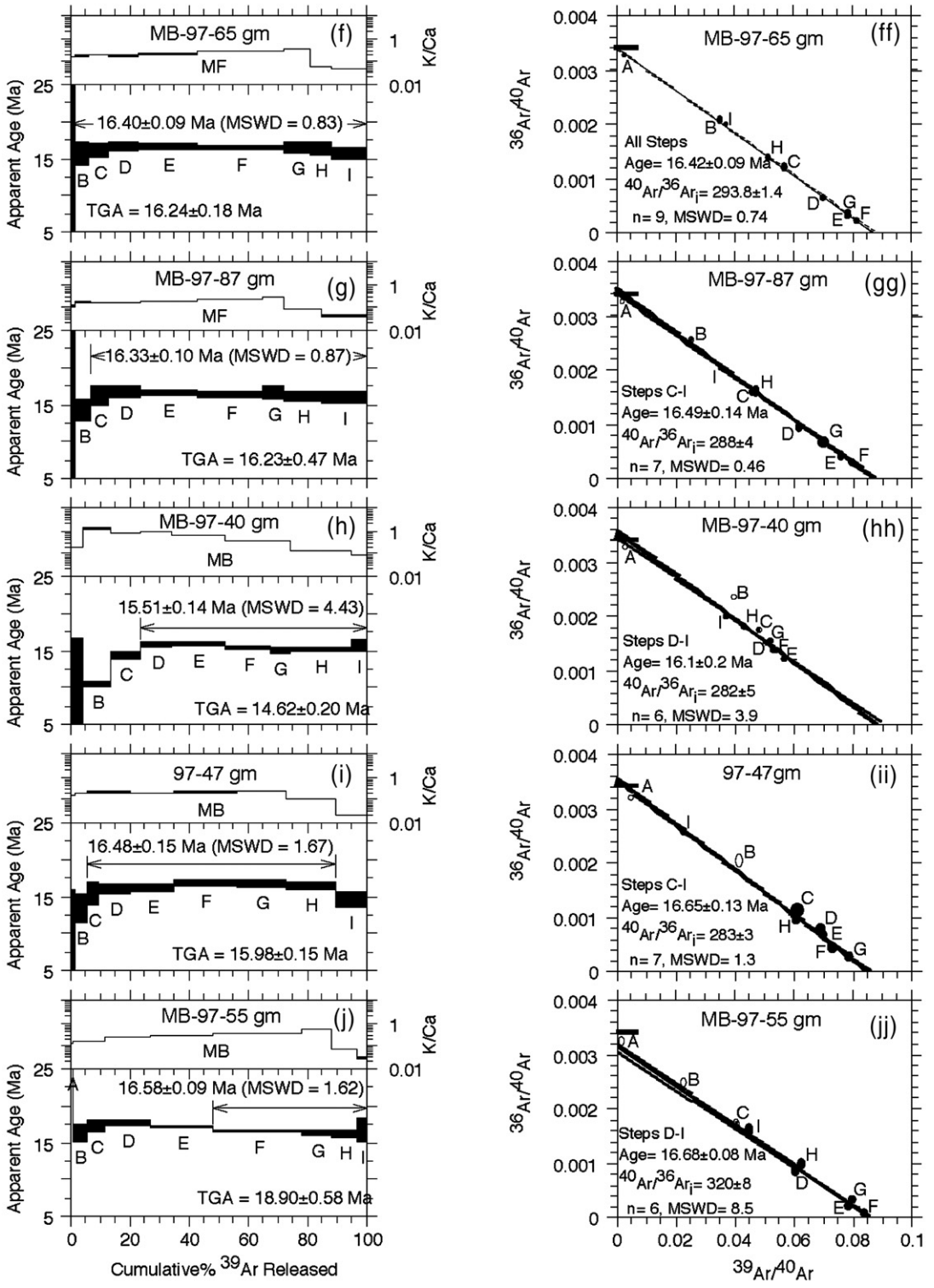

Fig. 2 (*continued*).

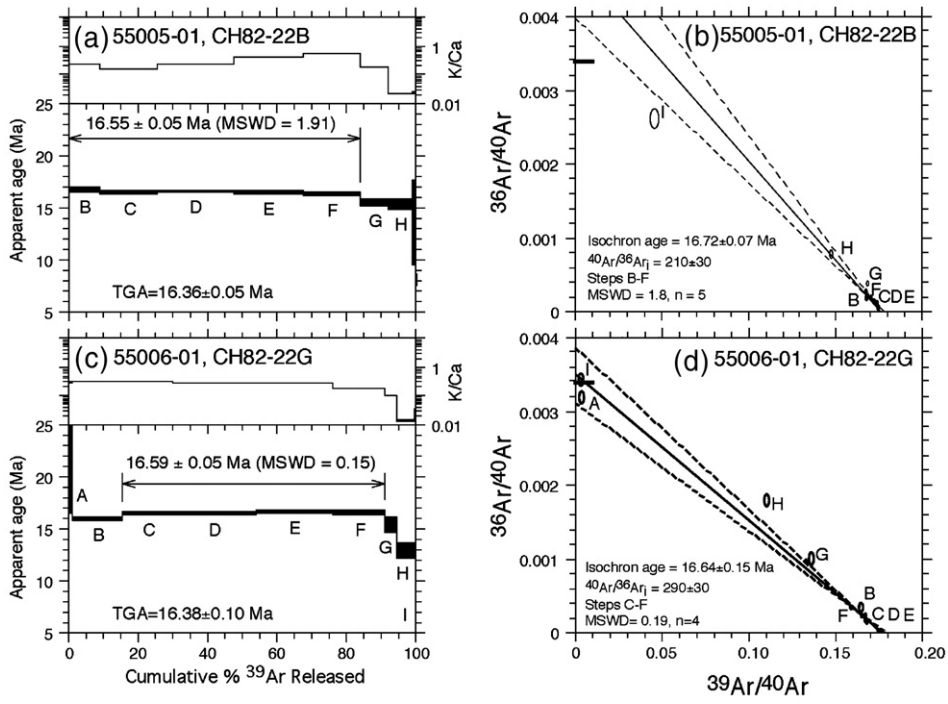

Fig. 3. a–d. $^{40}Ar/^{39}Ar$ age and K/Ca spectra and isotope correlation diagrams for dated lava flows from Steens Basalt at Steens Mountain. Errors are 1σ and isochron regressions use the method of York (1969). Sample CH82-22G is from the top flow whereas CH82-22B is from the 31st flow down from the top.

objective criteria. The disadvantage to this is that the pre-determined criteria may not always be applicable to all data sets in the study and there is no *a priori* way to know if the set criteria represent a geologically correct statistical model. Also, taking a fairly complex spectrum that happens to yield 3 consecutive steps that contain 50% of the total ^{39}Ar overlapping at 2σ and concluding it has a well-behaved plateau (i.e. Fleck et al., 1977) can alleviate the responsibility to look more closely at the rest of the spectrum that is disturbed. It is possible that this disturbance is also influencing the integrity of the "plateau." Perhaps all would agree that some sort of statistical test is required to justify an age assignment, but there is considerable disagreement on how to deal with data that violate (at some level) the predetermined statistical model. Isochron data have also been used to evaluate groundmass $^{40}Ar/^{39}Ar$ data (Singer and Pringle, 1996; Baksi, 1999; Heizler et al., 1999). Singer and Pringle (1996) suggest that isochron data of the chosen plateau steps should yield a $^{40}Ar/^{36}Ar_i$ value within error of the atmospheric $^{40}Ar/^{36}Ar$ value of 295.5. Baksi (1999) suggests the same; however he also requires the MSWD (mean square weighted deviate) value of the weighted regression to be less than 2.5. We view both of these criteria as useful approaches towards looking at the age spectrum data, but also recognize that if data chosen for the plateau age are statistically sound (i.e., normally distributed), the isochron data should yield the required atmospheric $^{40}Ar/^{36}Ar$ initial value (cf. Heizler et al., 1999). Also, choosing a cut-off value of 2.5 to distinguish between an isochron or errorchron might be misleading as the MSWD value needs to be evaluated based on the number of data points (Mahon, 1996).

For this study we are fortunate that many of the samples produce age spectra that yield at least 6 consecutive heating steps containing no less than 70% of the total ^{39}Ar released and have MSWD values that fall within the 95% confidence window for $n-1$ degrees of freedom (Figs. 2 and 3; Table 2). By any reasonable criterion, these groundmass samples can be considered as well behaved, despite having some discordance for early and late heating steps. Three samples (MB97-24; MB97-40; MB97-2) are more complex, but are still interpreted to yield useful data for determining eruption ages. MB97-2 reveals a significant age gradient that presumably records argon loss (Fig. 2b). This spectrum begins at about 5 Ma and climbs to about 16 Ma with the final 5 steps defining a normal distribution of ages with a weighted mean of 15.17±0.36 Ma and an MSWD of 1.90. However, these five steps only contain about 34%

Table 2
Summary of $^{40}Ar/^{39}Ar$ age results

Sample	Section location	Age analysis	Total steps	Steps used	$\%^{39}Ar$	MSWD	Age (Ma)	$\pm 2\sigma$ (Ma)
MB97-2	FFW	Plateau	9	5	34.3	1.90	15.17	0.36
MB97-40	MB	Plateau	9	6	76.3	4.43 [1]	15.51	0.28
MB97-32	R78N	Plateau	11	11	100.0	0.34	16.03	0.30
MB97-24	FFW	Plateau	9	6	77.0	4.37 [1]	16.06	0.36
MB97-25	R78N	Plateau	9	6	71.0	0.76	16.24	0.50
86-29	FFE	Plateau	9	6	88.8	1.34	16.31	0.20
MB97-87	MF	Plateau	9	7	92.9	0.87	16.33	0.20
CH82-22B	Steens Mt	Plateau	9	6	84.0	1.91	16.55	0.10
CH82-22G	Steens Mt	Plateau	9	4	75.6	0.15	16.59	0.10
MB97-65	MF	Plateau	9	8	98.1	0.90	16.40	0.18
MB97-47	MB	Plateau	9	6	84.4	1.67	16.48	0.30
MB97-55	MB	Plateau	9	4	51.5	1.62	16.58	0.18

Section location abbreviations are as follows: FFE, Folly Farm East; FFW, Folly Farm West; R78N, Route 78 North; MF, Miranda Flat; MB, Mickey Butte. Samples selected for geochronology were analyzed at the New Mexico Geochronology Research Laboratory via the incremental heating age spectrum method (see Appendix A for detailed information). Groundmass concentrates were used for each analysis with the exception of the coarsely plagioclase-phyric sample, MB97-32, where plagioclase was analyzed. All of the new plateau ages are interpreted to represent eruptive ages. The ages listed are calculated relative to FC-2 Fish Canyon Tuff sanidine interlaboratory standard at 28.02 Ma and errors include 0.2% (2σ) error in *J*.
[1] MSWD outside of 95% confidence window for $n-1$ degrees of freedom.

of the total ^{39}Ar released and we are not confident that the final heating steps have not also been disturbed by argon loss and therefore suggest that the assigned age represents a minimum age of eruption. Samples MB97-24 and MB97-40 yield very similar age spectra with climbing initial steps that reach a maximum before decreasing for the higher temperature steps (Fig. 2c, h). In both cases, combining steps D–I yield MSWD values of approximately 4.4 and fall outside the 95% confidence window. This suggests that these steps do not record a normal distribution of apparent ages and warrant some caution when considering these dates as representing eruption ages. In the case of MB97-24, steps D–I have a weighted mean age of 16.06±0.36 Ma with step H being the cause of the high MSWD (Fig. 2c; Appendix A; Argon data repository). It is possible that step H is simply a random statistical outlier that could be tested by additional analyses, or the discordance could be related to geological affects (argon loss) or irradiation-induced artifacts (^{39}Ar recoil). One alternative way to assign an age to this sample is to combine steps D–G to obtain a weighted mean age of 16.15± 0.30 Ma and MSWD of 2.72. This method uses greater than 50% of the ^{39}Ar released and produces an MSWD that falls within the 95% confidence window for 3 degrees of freedom. Additionally, steps E–G yield a weighted mean of 16.20±0.20 Ma and an MSWD of 1.09. These data are clearly a population, but only comprise 45.8% of the total ^{39}Ar. Because the 50% rule for the plateau segment is not upheld, workers such as Baksi (1999) would define this as a marginal plateau. Similar combinations of steps can be used to evaluate an age for MB97-40. For instance, the final 4 heating steps that contain about 48% of the total ^{39}Ar released yield an age of 15.21±0.20 Ma and an MSWD of 1.04. We choose to combine steps D–I that yield an age of 15.51± 0.28 Ma in the recognition that this discordance for this part of the spectrum could be caused by ^{39}Ar recoil redistribution. The main point of this discussion of age assignment is that there is no accepted (and perhaps there should not be) method to calculate eruption ages from somewhat disturbed spectra. It is however, important to evaluate different methods to see if these different methods might lead to age determinations that influence a geological interpretation. In the above three examples (MB97-24; MB97-40; MB97-2) the main observation is that the spectra seem to indicate argon loss and perhaps any age determined from these samples should be considered as minimum values for basalt eruption.

The remaining six Oregon Plateau samples are less disturbed. Two of the samples (MB97-65 groundmass and MB97-32 plagioclase) are flat over 100% of the ^{39}Ar released and presumably record accurate eruption ages (Fig. 2e, f). The final samples generally yield initial age gradients indicative of minor argon loss that are followed by significant plateau segments (Fig. 2a, c, d, g). The initial disturbance of the spectra is probably related to argon loss; however we suggest that the plateau segments are recording accurate eruption ages. The age spectrum for MB97-55 is slightly different compared to the other Oregon Plateau basalts in that it has some relatively old steps before decreasing to a well-defined

flat segment (16.58±0.18 Ma; MSWD=1.62) for the remaining four heating steps (Fig. 2j). This pattern could result from ^{39}Ar recoil and/or excess argon; however despite this complexity we suggest that the assigned age records an accurate eruption age.

The isotope correlation data from the Oregon Plateau basalts are consistent with the ages provided by the age spectra. In no case is the isochron age significantly different from the assigned plateau ages; however there are a couple of cases where initial trapped ^{40}Ar/^{36}Ar components differ slightly from atmosphere (e.g. Fig. 2cc, hh, ii, jj). In most of these cases the MSWD values are slightly elevated and perhaps are recording regression of heating steps with non-isochronous ages (i.e., age gradients) or are recording anomalous behavior related to ^{39}Ar recoil.

The two samples from Steens Mountain (CH82-22B and CH82-22G) are overall highly radiogenic and yield precise individual apparent ages (Fig. 3a, c; Appendix A; Argon data repository). Their spectra are somewhat different compared to the samples discussed above as they exhibit a slight age decrease across the spectrum with the final 10 to 20% of the ^{39}Ar released yielding steps with a more dramatic age drop. Especially in the case of CH82-22G, the spectrum looks like a classic ^{39}Ar recoil pattern with ^{39}Ar being displaced from relatively high K locations into low K locations that degas at high temperature (Fig. 3c). If recoil redistribution is the cause for the age spectra discordance, it could be argued that the integrated ages of 16.36±0.10 Ma for CH82-22B and 16.38±0.20 Ma for CH82-22G are the accurate eruptions ages. However both spectra also record well-defined plateau segments with apparent ages of 16.55±0.10 Ma and 16.59±0.10 Ma (Fig. 3a, c). A best age for these samples is aided by precise dating of sanidine from silicic volcanic rocks that stratigraphically overlie Steens Basalt just to the south of Steens Mountain in the Pueblo Mountains (the ~16.4 Ma tuff of Oregon Canyon; Perkins and Nash, 2002; Henry et al., 2006), which indicate that the Steens Mountain section is older than 16.5 Ma. Recently reported ages from Steens Basalt lava flows from within the Steens Mountain section (Jarboe et al., 2003, 2006) also agree with our results and further indicate that the plateau segment of our spectra is most accurate. Due to data clustering, the isochron data for these samples do not significantly enhance age assignment (Fig. 3b, d). At the 2-sigma confidence level the isochron ages recorded by the plateau steps are not distinguishable from the plateau ages, but may not be meaningful because of probable recoil issues. There are large errors on the initial trapped ^{40}Ar/^{36}Ar components due to the low number of heating steps and due to the high and fairly constant radiogenic yields of individual steps used to define the linear regressions. For these reasons we do not apply great significance to the trapped component values, but recognize that the apparent value of 210±60 (2σ) for CH82-22B is analytically less than the atmospheric value of 295.5, further suggesting possible recoil problems.

Eight and nine aliquots of CH82-22B and CH82-22G, respectively were step-heated in two or three increments (Figs. 4 and 5). These are the identical samples analyzed by Swisher et al. (1990) and we attempted to reproduce their results. Swisher et al. (1990) combined the "B" steps of the two-step spectra to obtain a precise weighted mean age for each sample. This method was utilized to remove the relatively non-radiogenic, disturbed low temperature gas prior to sample fusion and thus attainment of a more accurate age compared to simple total fusion analyses. Our analyses are very similar to those of Swisher et al. (1990) as the first heating step is relatively non radiogenic followed by a fusion step that is typically about 90% radiogenic (Figs. 4 and 5). The B-steps for CH82-22B yielded a weighted mean age of 16.48±0.06 Ma (MSWD=3.05). Eight of the nine B-steps from CH82-22G yield a well-defined (MSWD=1.22) weighted mean age of 16.46±0.06 Ma. Run number 55006-22 for CH82-22G yields an anomalously old apparent age of 17.27±0.26 Ma and also has a low radiogenic yield of only 43.9% (Appendix A; Argon data repository). Perhaps this aliquot contains a phenocryst with excess argon or has an incompletely degassed xenocryst that is resulting in an inaccurate result. The 16.46 Ma B-step fall between the plateau ages (~16.56 Ma) and the total gas ages (~16.36 Ma) obtained from the higher resolution spectra (Fig. 3) and are consistent with the low-resolution homogenization of the overall age variations observed in the higher resolution age spectrum runs.

2.1. Eruption ages and normalization of published results

For all but sample MB97-2 of the Oregon Plateau lava flows, the assigned plateau or preferred ages are interpreted to record accurate eruption ages. The high degree of argon loss evident in MB97-2 (Fig. 2b) requires a cautious interpretation and the assigned age of 15.17±0.36 Ma perhaps represents a minimum age for eruption. In all cases the eruption ages are consistent with stratigraphic relationships (see next section) attesting to the robustness of the data set.

Regional comparisons for the basalt geochronology reported by other workers are hampered somewhat by difficulty in normalizing all data to a common standard. Below we present data from the area that is compiled

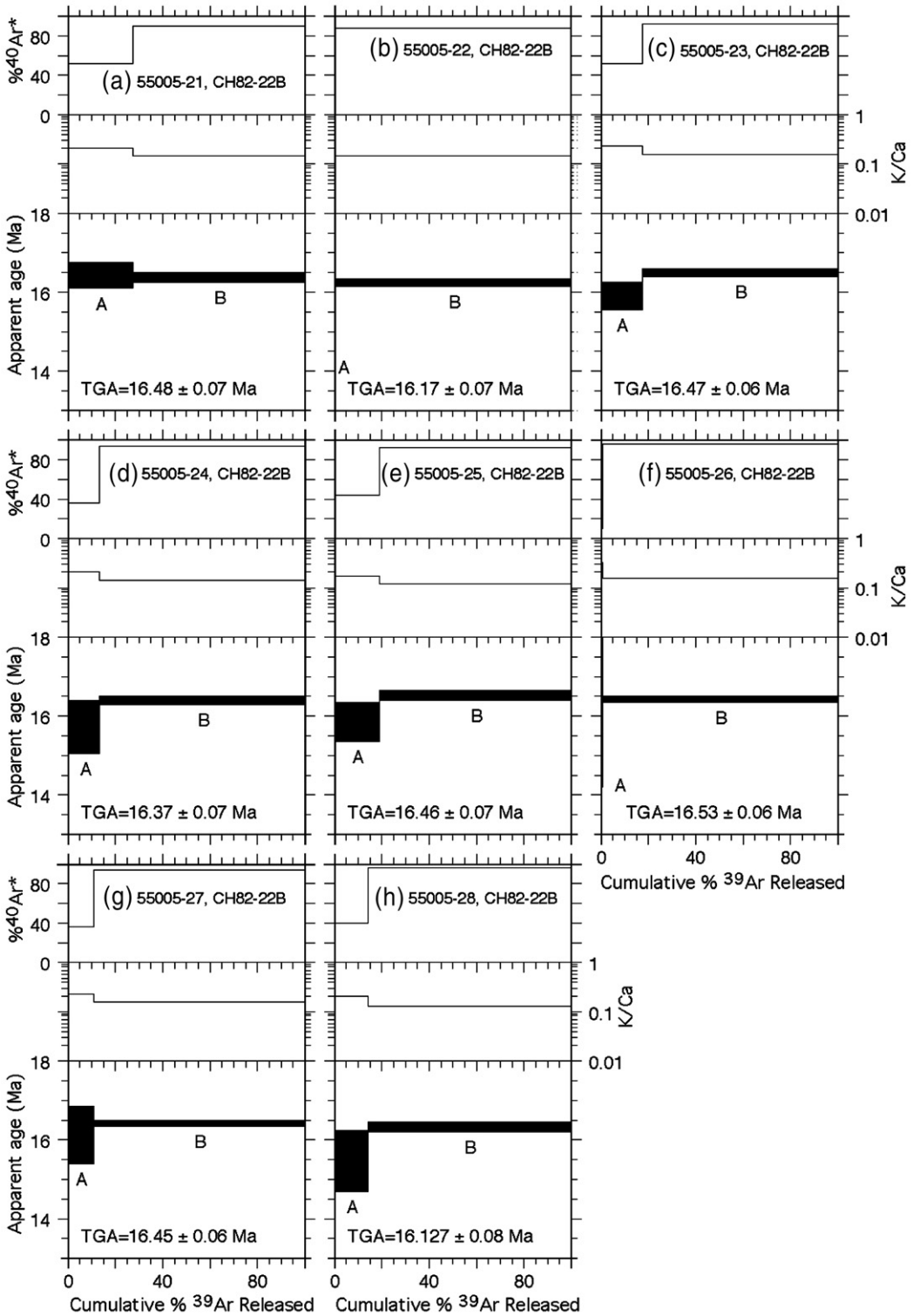

Fig. 4. $^{40}Ar/^{39}Ar$ age and K/Ca spectra diagrams for low resolution laser heating analyses for Steens Basalt at Steens Mountain. Errors are 1σ. Sample CH82-22B is from the 31st flow down from the top.

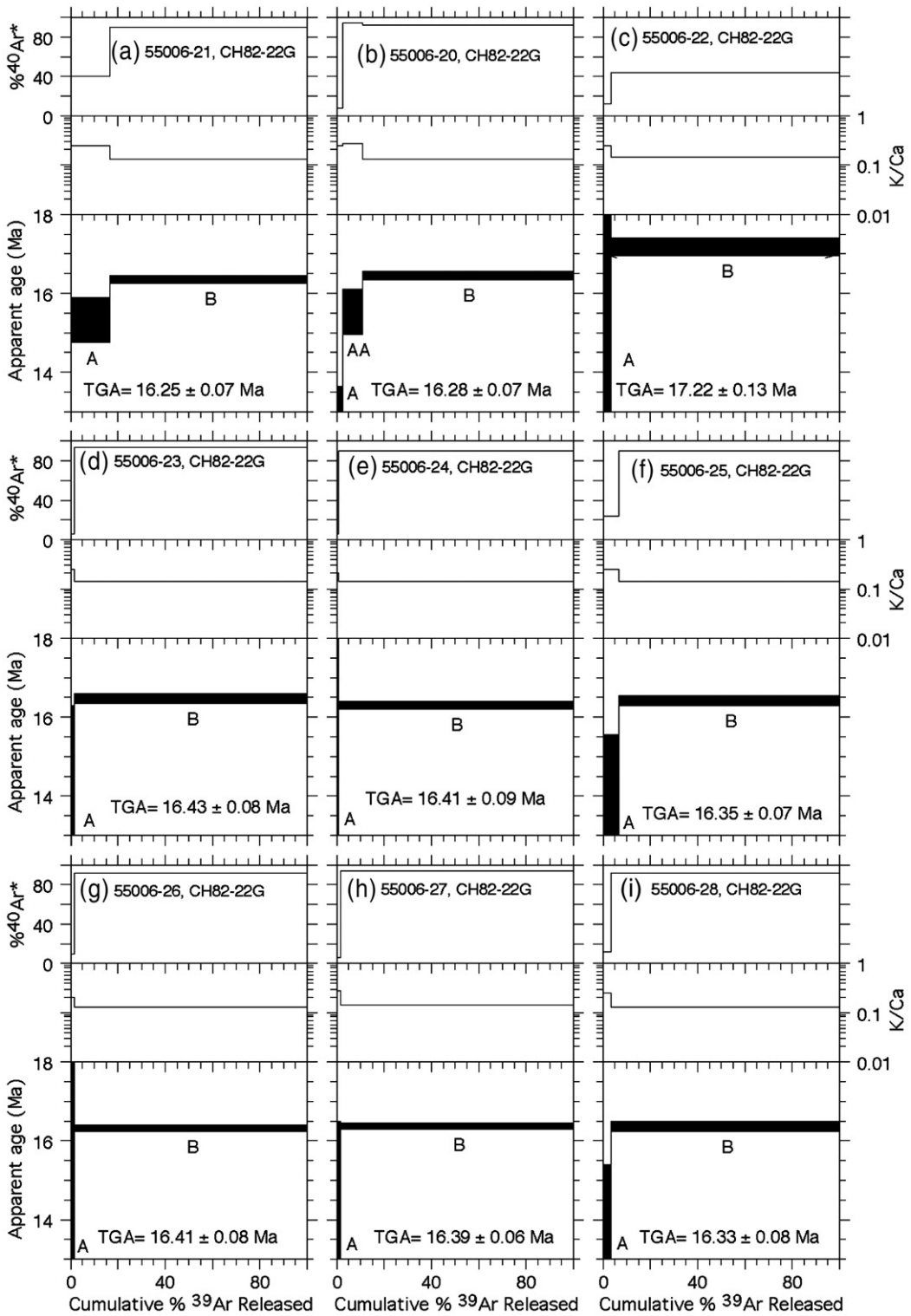

Fig. 5. $^{40}Ar/^{39}Ar$ age and K/Ca spectra diagrams for low resolution laser heating analyses for Steens Basalt at Steens Mountain. Errors are 1σ. Sample CH82-22G is from the top flow.

from a variety of publications (Table 3). This compilation shows that at least 5 different fluence monitors were used with only some having well determined intercalibration values (e.g. Renne et al., 1998). We have attempted to normalize all data to Fish Canyon (FC) tuff sanidine at 28.02 Ma such that discussion of the ages can be done from a consistent platform. Recall that we have also analyzed two samples from Steens Mountain so that our data is more readily compared to previous work by Swisher et al. (1990), Baksi and Farrar (1990), and Baksi et al. (1991). All of these studies suggest that a significant number of the Steens Mountain lavas were erupted over a short interval and/or that the N/R paleomagnetic transition at Steens Mountain was established within the resolution of the ages below and above the transition. The relative duration (<0.1 Ma) of the reversal is agreed upon by all datasets, however the reported age for it varies by about 0.5 Ma. Swisher et al. (1990) dated the top flow and the 31st down from the top (both stratigraphically higher than the N/R reversal) and obtained ages of 16.583±0.048 Ma and 16.589±0.022 Ma, respectively. Baksi and Farrar (1990) report plateau ages of 16.06±0.10 Ma and 16.08±0.12 Ma for transitional basalts at Steens Mountain. Baksi et al. (1991) dated 11 samples (2 above, 2 below and 7 within the transition zone, all within the upper 450 m of the ~900 to 1000 m section; Mankinen, personal communication) and found no resolvable age difference and report an age for all samples at 16.2±0.1 Ma.

Each of these studies used a different fluence monitor that is likely contributing to some of the apparent discrepancies (Table 3). Our Steens Mountain samples (CH82-22G, CH82-22B) are identical to those analyzed by Swisher et al. (1990) with sample preparation also being identical (Table 1). Our preferred eruption ages are 16.59±0.10 Ma for CH82-22G (top flow) and 16.55±0.10 Ma for CH82-22B (31st down from top). Like previous studies, we cannot resolve an age difference between individual flows, and at first inspection these ages are identical to those reported by Swisher et al. (1990). However, considering that they used a basalt flux monitor standard that was internally calibrated to FC sanidine at 27.84 Ma (Swisher, personal communication) their ca. 16.59 Ma reported ages become 16.70 Ma and are about 0.1 to 0.15 Ma older than our preferred eruption age. Because the Swisher et al. (1990) data only appear in an abstract and were monitored with a basalt flux monitor with uncertain intercalibration with Fish Canyon sanidine we suggest that the Swisher et al. (1990) age be abandoned as a robust absolute age for the Steens Basalt exposed at Steens Mountain. Their highly precise results are still very useful for documenting the relative duration of eruptions at Steens Mountain.

The other pertinent published data from Steens Mountain come from Baksi and Farrar (1990) and Baksi et al. (1991). The Baksi and Farrar (1990) data of 16.06±0.10 Ma and 16.08±0.12 Ma combine to yield a weighted mean of 16.07±0.08 Ma. This age is relative to SB-3 biotite at 162.9 Ma which is intercalibrated with FC sanidine at 27.57 Ma (Lanphere and Baadsgaard, 2001). Therefore the Baksi and Farrar (1990) age of 16.07±0.08 Ma relative to FC at 28.02 Ma becomes 16.33±0.08 Ma and is about 0.25 Ma younger than our preferred eruption age. The 16.2±0.1 Ma result of Baksi et al. (1991)

Table 3
Summary of new and published Oregon Plateau flood basalt radiometric ages

Location	Unit	Range or weighted mean age (Ma±2σ)	Type (K–Ar or $^{40}Ar/^{39}Ar$)	Fluence monitor and age	Ages relative to FC at 28.02 Ma (±2σ)
Regional OP[1]	Oregon Plateau basalt	17±1 to 14±1	K–Ar		
Pueblo Mts.[2]	Oregon Plateau basalt	17.0±0.3 to 16.0±0.4	K–Ar		
Steens Mountain[3]	Steens Basalt	16.58±0.10 to 16.59±0.04	$^{40}Ar/^{39}Ar$	BCR-2 basalt, 15.6 Ma[11]	16.70±0.04[10]
Steens Mountain[4]	Steens Basalt	16.20±0.20	$^{40}Ar/^{39}Ar$	Hbgr3 hornblende, 1071 Ma	16.30±0.20
Steens Mountain[5]	Steens Basalt	16.06±0.20 to 16.08±0.24	$^{40}Ar/^{39}Ar$	SB-3 biot, 162.9 Ma	16.33±0.16[10]
Malheur Gorge[6]	Hunter Creek Basalt	15.8±0.6	$^{40}Ar/^{39}Ar$	GA1550 biot, 98.8 Ma	15.8±0.6
Malheur Gorge[6]	Birch Creek Basalt	15.7±0.1	$^{40}Ar/^{39}Ar$	GA1550 biot, 98.8 Ma	15.7±0.1
Malheur Gorge[6]	Upper Pole Creek	16.8±0.6 to 15.2±5.6	$^{40}Ar/^{39}Ar$	GA1550 biot, 98.8 Ma	16.8±0.6 to 15.2±5.6
Malheur Gorge[6]	Lower Pole Creek	17.0±1.6 to 15.8±5.6	$^{40}Ar/^{39}Ar$	GA1550 biot, 98.8 Ma	17.0±1.6 to 15.8±5.6
Owyhee Mts.[7]	Oregon Plateau basalt	16.10±0.17	$^{40}Ar/^{39}Ar$	FC san, 27.84 Ma	16.20±0.17
SC volcanic field[8]	Oregon Plateau basalt	16.73±0.04 to 14.35±0.38	$^{40}Ar/^{39}Ar$	FC san, 28.02 Ma	16.73±0.04 to 14.35±0.38
Steens Mountain[9]	Steens Basalt	16.59±0.10 to 16.55±0.10	$^{40}Ar/^{39}Ar$	FC san, 28.02 Ma	16.59±0.10 to 16.55±0.10
Steens Mt. vicinity[9]	Oregon Plateau basalt	16.58±0.18 to 15.51±0.28	$^{40}Ar/^{39}Ar$	FC san, 28.02 Ma	16.58±0.18 to 15.51±0.28

[1]Hart and Carlson (1985), [2]Hart et al. (1989), [3]Swisher et al. (1990), [4]Baksi et al. (1991), [5]Baksi and Farrar (1990), [6]Hooper et al. (2002), [7]Shoemaker and Hart (2003), [8]Brueseke and Hart (in press) (SC, Santa Rosa–Calico), Brueseke et al. (2003), [9]this study; [10]weighted means were calculated from age ranges and then normalized to 28.02 Ma; [11]information of flux monitor provided by C. Swisher.

was reported relative to Hbgr3 hornblende with an assigned age of 1071 Ma. Personal communication with Chris Hall at the University of Michigan reports that Hbgr3 intercalibrates well with Mmhb-1 hornblende at 520.4 Ma, the latter which has been intercalibrated by Deino and Potts (1990) with FC sanidine at 27.84 Ma. Thus, the 16.2±0.1 Ma result of Baksi et al. (1991) becomes 16.30±0.10 Ma relative to FC at 28.02 Ma. Thus, the Baksi and Farrar (1990) and the Baksi et al. (1991) results are internally consistent, but significantly lower than our new data, Swisher et al.'s (1990) data, and in contradiction to the feldspar ages reported by Jarboe et al. (2003, 2006) and Henry et al. (2006). There are likely many reasons for overall variability between all of the Steens age assignments and intercalibration of standards is perhaps the main problem. At present, we consider the plateau ages reported here to be the best available eruption age for Steens Mountain as the data are the most modern, of highest resolution, and were analyzed relative to one of the most well studied and characterized fluence monitors.

3. Stratigraphic results

Flood basalt lava flows crop out throughout the southern Oregon Plateau, but are best exposed in the vicinity of Steens Mountain (Fig. 1a and b). Steens Mountain and its southern extension the Pueblo Mountains, delineate an ~130 km north–northeast trending Cenozoic fault scarp. In contrast to CRBG lava flows, Steens Basalt (Oregon Plateau) lava flows are thinner (~1 to 12 m versus ~50+ m thick) and typically show little to no columnar joint development. Steens Basalt lava flows are also commonly compound, consisting internally of flow lobes with rubbly and brecciated flow surfaces. These lava flows vary petrographically from aphyric flows and flow packages to extremely plagioclase-phyric (dominated by ~1 to 4 cm plagioclase crystals) flow packages and also include sparsely plagioclase phyric textured lava flows (hereafter termed intermediate-plagioclase), independent of stratigraphic position or geographic location. While interflow sediments are sparse, they do exist within packages of lava flows investigated in this study. In some cases the interflow horizons have been interpreted as regionally exposed tuffs by previous workers and have been used to mark the upper stratigraphic boundary of the Steens Basalt and separate it from petrographically similar basaltic lava flows (Sherrod et al., 1989; Johnson, 1995). While useful in field mapping, these boundaries are not supported by petrographic or chemical constraints from the lava flows themselves (Brueseke and Hart, 2002).

In order to assess the chronological implications of these observations, five new stratigraphic sections (~100 to ~350 m thick exposures) in proximity to Steens Mountain (Figs. 1b and 6) were investigated in detail. Section locations were chosen to maximize the number of lava flows exposed in continuous stratigraphic context, thereby allowing flow-by-flow description and sampling. In the field, no attempt was made to discern discrete flow packages. However, based on up-section petrographic and chemical variations it is apparent that many of the "individual flows" that were sampled are from discrete flow packages of similar material that were likely emplaced as inflated pahoehoe lobes. Geographically, two of the sections lie on or within the main Steens Mountain fault scarp ~50 km north of the type section and two additional sections lie less than 15 km across the Alvord Valley from the summit of Steens Mountain (Fig. 1b).

3.1. Folly Farm East

The Folly Farm East section lies in the northwest quarter of section 4 of the Johnny Creek NW quadrangle and extends into the Folly Farm quadrangle (T30S, R37E). At this location, ~271 m of section is exposed and 30 individual lava flows were sampled (Fig. 6). While all three Steens Basalt petrographic types are present (aphyric, intermediate-plagioclase, plagioclase-phyric), this section is dominated by intermediate-plagioclase bearing lava flows. Additionally, it appears that most of these lava flows were emplaced as lobes, capped by ~3 to 12 m of aphyric lava flows. The intermediate-plagioclase and aphyric package is repeated three times and may represent the eruption of a stratified magmatic system, similar to what is present throughout the Steens Basalt type section (Gunn and Watkins, 1970; Stewart, 1992). Approximately 58 m of plagioclase-phyric lava flows occur near the top of the section and comprise the thickest flow unit exposed at this location. In addition to the aphyric lava flows interspersed throughout the section, two zones of brecciated and blocky lava flows are exposed near its base. The basal lava flow exposed at this location yields a $^{40}Ar/^{39}Ar$ age of 16.31±0.20 (Fig. 6; Table 2). Additionally, unpublished paleomagnetic data from this section indicate that the entire package of lava flows erupted during a normal geomagnetic interval (Smith, 1987).

3.2. Folly Farm West

The Folly Farm West section lies in sections 14 and 23 of the Lambing Canyon quadrangle (T29S, R36E). Here,

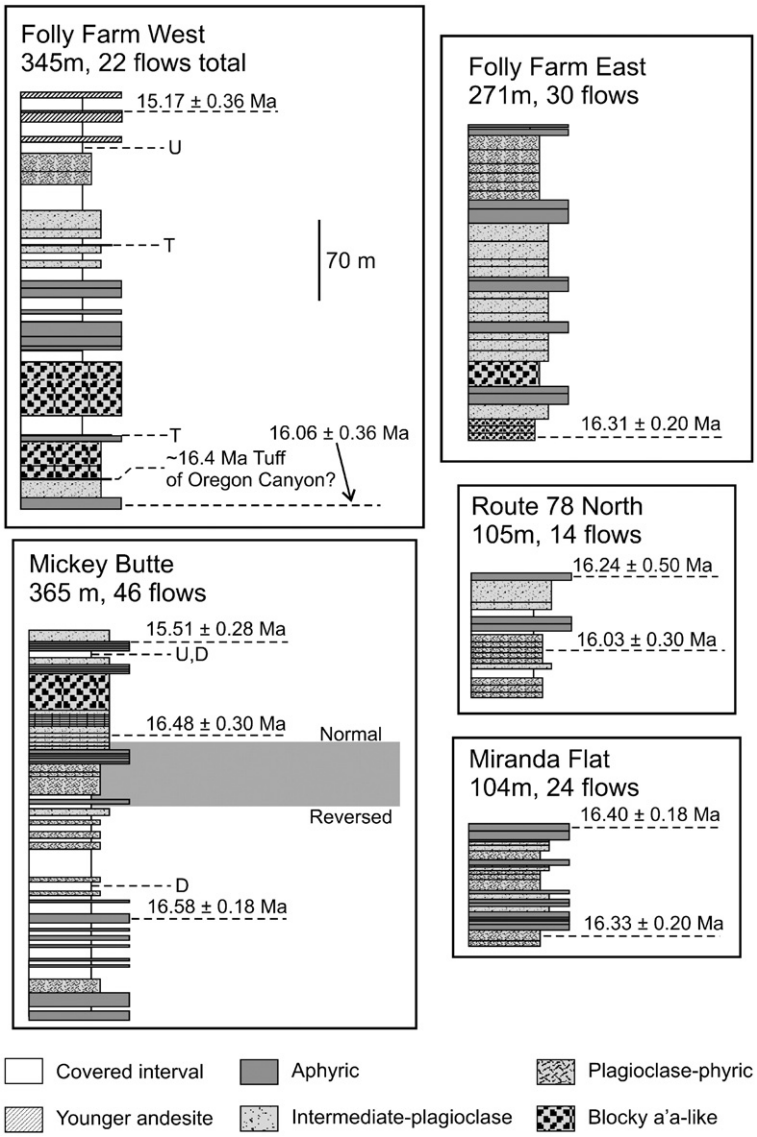

Fig. 6. Petrographic and stratigraphic relationships of sampled sections. For details of each stratigraphic section, see discussion under Stratigraphic results section. $^{40}Ar/^{39}Ar$ ages obtained at each section are illustrated and each dashed horizontal line either indicates a dated lava flow or other horizon of geologic interest (T, tuffaceous/sedimentary horizon; U, unconformity or disconformity; D, dike). The entire section at Folly Farm East consists of normal polarity lava flows and the reverse to normal polarity transition at Mickey Butte is shown at its approximate stratigraphic level. The scale near the Folly Farm West section is applicable to all sections.

22 lava flows are present and each was sampled (Fig. 6). Along with the lava flows/flow units, three tuffaceous/sedimentary horizons are present within this package. Disconformably overlying the uppermost exposed flood basalt flow are four ~3 to 6 m thick aphyric, tholeiitic andesite lava flows. The second andesite flow down section yields a minimum $^{40}Ar/^{39}Ar$ age of 15.17± 0.36 Ma. Compositionally similar flows have been documented regionally (e.g. Rytuba and McKee, 1984; Mankinen et al., 1987), but the relationship of these lava flows with the older flood basalts and/or local eruptive systems warrants further investigation. Because of their highly evolved nature, we exclude these from further discussion throughout the remainder of this paper. The remaining 300 m of the ~345 m section is composed of aphyric, intermediate-plagioclase, and plagioclase-phyric textured mafic lava flows that can be grouped into five flow units based on petrography and chemical variations. The basal lava flow from the lowermost unit yields a $^{40}Ar/^{39}Ar$ age of 16.06±0.36 Ma.

Approximately 27 and 67 m above the lowest exposed lava flow lie two thin tuffaceous horizons, both less than 1 m thick. Additionally, a third, thinner tuffaceous horizon crops out ~80 m from the top of the flood basalt section within a package of intermediate-plagioclase textured lava flows. The lowermost exposed tuffaceous horizon may be correlative with the ~16.4 Ma tuff of Oregon Canyon (Perkins and Nash, 2002; Henry et al., 2006). The presence of these tuffaceous and sedimentary horizons indicate periods of local magmatic quiescence, followed by later volcanism.

3.3. Route 78 North

The Route 78 North section lies in the northwest quarter of section 30 of the Folly Farm quadrangle (T28S, R37E). Fourteen lava flows are present and all were sampled in ~105 m of section exposed in a fault block within the Brothers fault zone (Fig. 6). This section is dominated by plagioclase-phyric lava flows in its lower half. Plagioclase separates extracted from a lava flow exposed approximately in the middle of the section yield a $^{40}Ar/^{39}Ar$ age of 16.03±0.30 Ma. Five intermediate-plagioclase to aphyric textured lava flows are exposed in the upper ~50 m of section. The uppermost exposed lava flow of this group and the section yields a $^{40}Ar/^{39}Ar$ age of 16.24±0.50 Ma, constraining the age of this section to <16.3 Ma.

3.4. Miranda Flat

This section lies directly across Miranda Flat from the main Steens Mountain fault scarp and is in the western half of section 4 of the Miranda Flat quadrangle (T33S, R35E). Twenty-four lava flows were sampled in succession from 104 m of section (Fig. 6). Similar to the upper portion of the Mickey Butte section (see below), lava flows exposed here are much thinner (~5 m average) than at other sampled sections. Exposed lava flows range from aphyric to plagioclase-phyric in texture and the upper half of the section is composed of two ~30 m packages that grade up-section from plagioclase-phyric, to intermediate-plagioclase, to aphyric lava flows. At this location, the uppermost lava flow yields a $^{40}Ar/^{39}Ar$ age of 16.40±0.18 Ma, while the second lava flow from the base of the section yields a $^{40}Ar/^{39}Ar$ age of 16.33±0.20 Ma.

3.5. Mickey Butte

This section lies along the western flank of Mickey Basin, a northern extension of the Alvord Valley in the southeast quarter of section one of the Mickey Springs quadrangle (R35E, T33S). From the valley floor to the summit of Mickey Butte is ~608 m of section, of which, ~365 m was investigated (Fig. 6). Within this section 19 of 46 lava flows were sampled. Like the other sections, petrographic type was variable, though intermediate-plagioclase lava flows dominate the upper portion of the sampled section. When variations do occur, they appear to represent packages of petrographically similar flows, but do not exhibit the apparent cyclicity of petrographic types present at Folly Farm East or Miranda Flat. Individual lava flows range from ~1 to ~24 m in thickness and the upper portion of this section is dominated by thin (~<5 m average) sheet-like lava flows that are interpreted as near-vent facies.

Two features set Mickey Butte apart from the other sections: (1) the presence of local dikes and (2) a distinct difference in eruptive age between the upper and lower portions of the investigated section. Three dikes are exposed at the Mickey Butte section and their average trend is N13°E. The best exposed dike cuts through ~250 m of section and appears to feed lava flows in the upper, unsampled portion of the section. The other dikes cut through the basal portion of the section and are all petrographically similar to Steens Basalt lava flows. Three lava flows from this section were selected for $^{40}Ar/^{39}Ar$ analyses. Two of these lava flows, exposed near the bottom and upper portion of the package yield similar ages of 16.58±0.18 Ma and 16.48±0.30 Ma, respectively. The lava flow directly underlying the uppermost sampled flow yields a $^{40}Ar/^{39}Ar$ age of

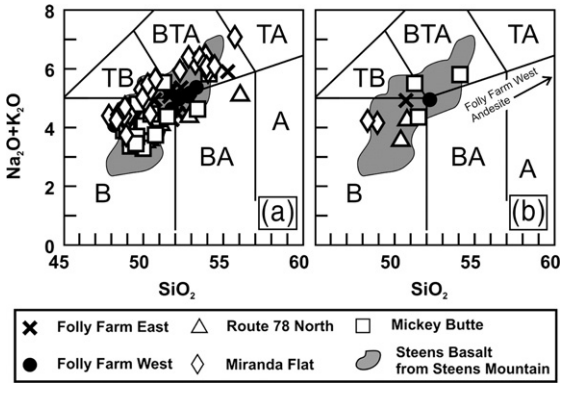

Fig. 7. (a) Total alkali vs. silica diagram (LeBas et al., 1986) illustrating similarities between Steens Basalt lava flows from Steens Mountain and Oregon Plateau flood basalts presented in this study. B=basalt; BA=basaltic andesite; A=andesite; TB=trachybasalt; BTA=basaltic trachyandesite; TA=trachyandesite. (b) Same diagram with only the newly dated samples illustrated. All values on both diagrams in wt.%.

Table 4
Major and trace element geochemical data for dated Oregon Plateau lava flows

Sample	MB97-2	MB97-24	MB97-25	MB97-32	MB97-40	MB97-47	MB97-55	MB97-65	MB97-87	86-29	CH82-22B	CH82-22G
SiO_2	59.46	51.22	49.39	50.21	53.36	50.73	51.17	47.98	47.38	50.39	47.30	47.30
TiO_2	2.03	2.55	1.93	2.32	2.56	2.58	2.28	2.09	2.06	2.14	2.20	2.38
Al_2O3	13.45	13.18	15.16	17.32	14.40	14.97	15.17	15.92	16.30	15.68	16.40	15.70
Fe_2O_3	8.86	14.78	13.18	11.83	12.11	13.65	12.52	13.49	13.43	13.15	13.90	15.10
MnO	0.14	0.22	0.19	0.16	0.19	0.20	0.15	0.18	0.18	0.20	0.19	0.19
MgO	2.13	4.16	6.09	4.00	3.46	4.33	5.15	6.24	6.34	4.88	5.09	5.73
CaO	5.51	7.64	9.11	9.18	6.78	7.16	8.76	8.53	8.77	8.35	8.79	8.25
Na_2O	3.28	3.34	2.88	3.25	3.42	3.56	3.16	3.16	3.25	3.62	3.00	3.14
K_2O	2.80	1.52	0.59	0.95	2.32	1.90	1.17	0.92	0.89	1.27	1.29	0.99
P_2O_5	0.39	0.36	0.31	0.35	0.65	0.64	0.56	0.41	0.32	0.44	0.37	0.34
LOI	1.08	−0.06	0.21	0.28	1.05	1.26	1.11	0.42	0.40	1.50	0.31	0.47
Total	99.13	98.91	99.04	99.85	100.30	100.98	101.20	99.34	99.32	101.62	98.84	99.59
Ba	1226	561	419	397	742	314	525	374	345	620	–	–
Ce	64	38	30	36	62	38	46	27	31	52	–	–
Co	40	41	45	36	28	50	40	49	52	38	–	–
Cr	25	31	36	33	11	43	3	44	23	–	60	70
Cu	17	244	25	92	162	90	41	212	177	62	–	–
Ga	20.6	26.1	25.1	27.4	25.0	24.6	24.2	24.2	24.0	23.5	–	–
La	30	20	16	17	33	14	25	14	12	27	–	–
Nb	15.5	11.6	14.9	13.4	17.6	14.3	15.9	10.7	10.4	14.2	–	–
Ni	12	22	27	53	12	118	48	129	136	66	–	–
Pb	15	9	5	6	11	5	5	5	4	–	–	–
Rb	78	35	12	22	53	8.2	18	15	13	29	13	14
Sc	25.6	33.5	27.3	25.6	24.9	29.3	23.9	27.7	27.7	–	–	–
Sr	333	397	463	498	461	479	511	490	532	514	553	476
Th	8.2	4.6	3.4	4.4	7.8	2.6	5.4	4.3	3.8	5.1	–	–
U	2.8	1.5	1.6	1.2	1.6	0.6	1.1	0.2	1.3	0.4	–	–
V	330	406	254	265	275	334	299	350	352	212	–	–
Y	44	37	25	30	43	30	32	29	29	36	–	–
Zn	131	118	117	103	132	127	134	114	111	109	–	–
Zr	282	194	135	166	270	171	197	151	144	213	140	100

Note: Major element concentrations are reported as weight percent oxides and expressed as raw data; trace element concentrations are reported in ppm. Major elements were analyzed by the techniques outlined in Katoh et al. (1999) at Miami University by DCP-AES (Direct Current Argon Plasma Atomic Emission Spectrometry), except for CH82-22B and G. Trace elements were analyzed by XRF (X-ray fluorescence) at Franklin and Marshall College by techniques outlined in Mertzman (2000) except for CH82-22B and G. Major and trace element compositions for CH82-22B and G were determined by XRAL Ltd. by XRF and originally reported in Carlson and Hart (1987).

15.51±0.28 Ma, suggesting the presence of a within-section unconformity. Hook (1981) investigated the entire Mickey Butte section and his work indicates that all but the upper ~45 m of the ~243 m of section not investigated in this study is composed of lava flows that he identified as identical to those exposed down section. This implies that at least a 550 m thick package of flood basalt lava flows is exposed at Mickey Butte. Hook (1981) also documented a normal over reverse paleomagnetic polarity change at this location and its approximate location within the Mickey Butte section is shown in Fig. 6. Hook (1981) suggested that this N/R reversal was correlative to the Steens Mountain reversal and this interpretation agrees with our results, indicating that this polarity change is the same reversal. All of these data combined appear to indicate the presence of at least a local magmatic hiatus near the top of the sampled section and indicate that the Mickey Butte region was characterized by local eruptive activity.

3.6. Steens Mountain

In comparison to the newly sampled sections, the Steens Basalt type section at Steens Mountain is much thicker (~900 to 1000 m) and exposes at least 75 to 100 lava flows (Gunn and Watkins, 1970; Johnson et al., 1998). Exposed lava flows are petrographically similar to flows sampled in this study and range from aphyric to plagioclase-phyric varieties (Gunn and Watkins, 1970). These lava flows also vary petrographically throughout the section and at the type section, meter scale flow packages of extremely plagioclase-phyric lava flows are

often interbedded with aphyric varieties (Gunn and Watkins, 1970; Mankinen et al., 1985). The age results of these Steens Mountain basalts are discussed above and it is here suggested that the upper ~450 m of the section falls within a tight age range of 16.57±0.04 Ma. The fact that only the top ~450 m of the section is well dated leaves open the possibility that older lava flows are present; however, the presence of older lava flows would be at odds with the rapid eruptive rates calculated by earlier workers for the entire ~900 to 1000 m section (Baksi et al., 1967; Gunn and Watkins, 1970; Grommé et al., 1985; Mankinen et al., 1985; Mankinen et al., 1987).

In summary, the presence of dikes, local near-vent facies, and the chronologic differences that reveal the intra-section unconformity at Mickey Butte, help demonstrate that basaltic volcanism in the region peripheral to Steens Mountain was complex. Furthermore, the distal facies of regional silicic pyroclastic units and thin interflow sedimentary zones found at Folly Farm West separate dissimilar geochemical and petrographic flow packages. These data combined with the new $^{40}Ar/^{39}Ar$ ages demonstrate that periods of mafic volcanic inactivity were present over at least an ~1 m.y. duration, as local volcanism stopped and then resumed at different eruptive loci. We feel that the presence of multiple eruptive centers and irregular paleorelief created by pre- and syn-volcanic extension has resulted in extensive interfingering of these lava flows.

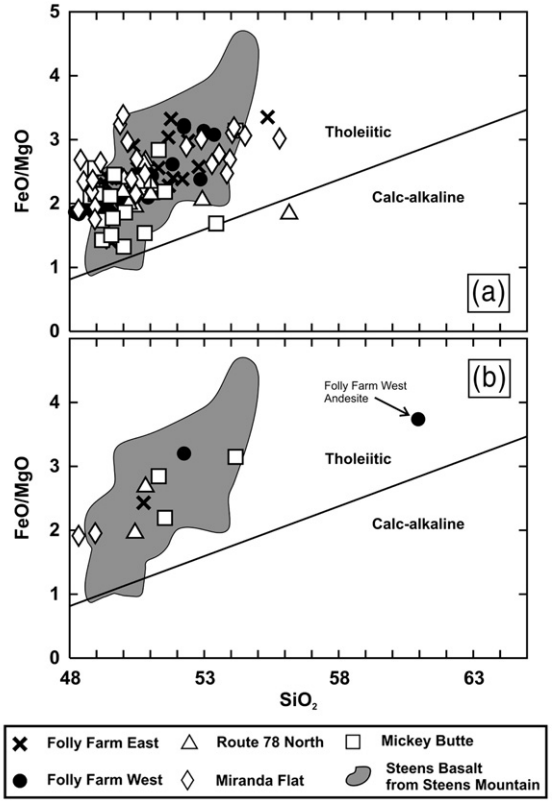

Fig. 8. (a) FeO/MgO vs. silica diagram of Miyashiro (1974) illustrating the tholeiitic vs. calc-alkaline affinities of Steens Basalt lava flows from Steens Mountain and Oregon Plateau flood basalts presented in this study. (b) Same diagram with only the newly dated samples illustrated. SiO_2 is reported as wt.%.

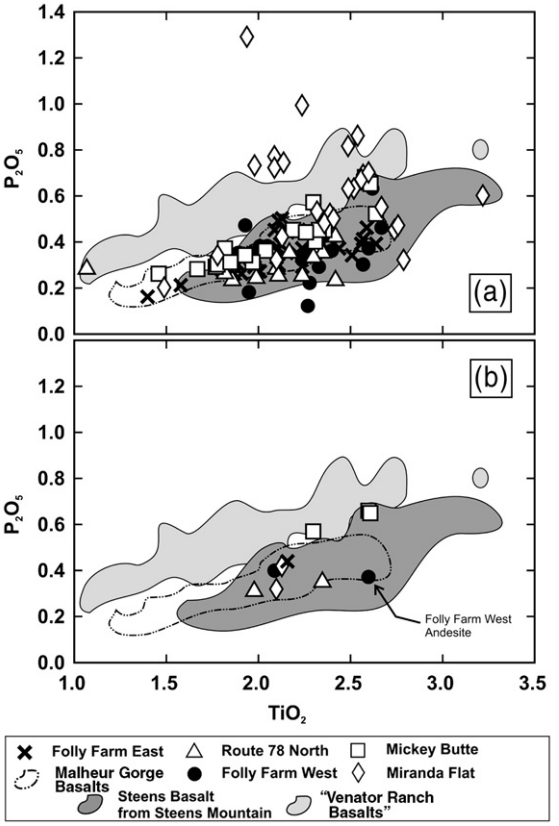

Fig. 9. (a) Plot of TiO_2 vs. P_2O_5 (wt.%) illustrating compositional variation of Oregon Plateau flood basalts from this study and Steens Basalt lava flows from Steens Mountain (Johnson et al., 1998). Also depicted are fields for the Malheur Gorge-region tholeiitic flood basalts (Camp et al., 2003) and Venator Ranch basalts (Camp et al., 2003). Notice that most of the Oregon Plateau flood basalts from this study fall along the array defined by the Steens Basalt from Steens Mountain. Eight samples from this study plot above the Venator Ranch field, defining a local subgroup exposed at the Miranda Flat section. (b) Same diagram with only the newly dated samples illustrated.

4. Chemostratigraphy of Oregon Plateau flood basalts

The chemical diversity of Oregon Plateau flood basalts from locations peripheral to Steens Mountain has received little attention, even though the geochemical diversity of Steens Basalt lava flows has been well

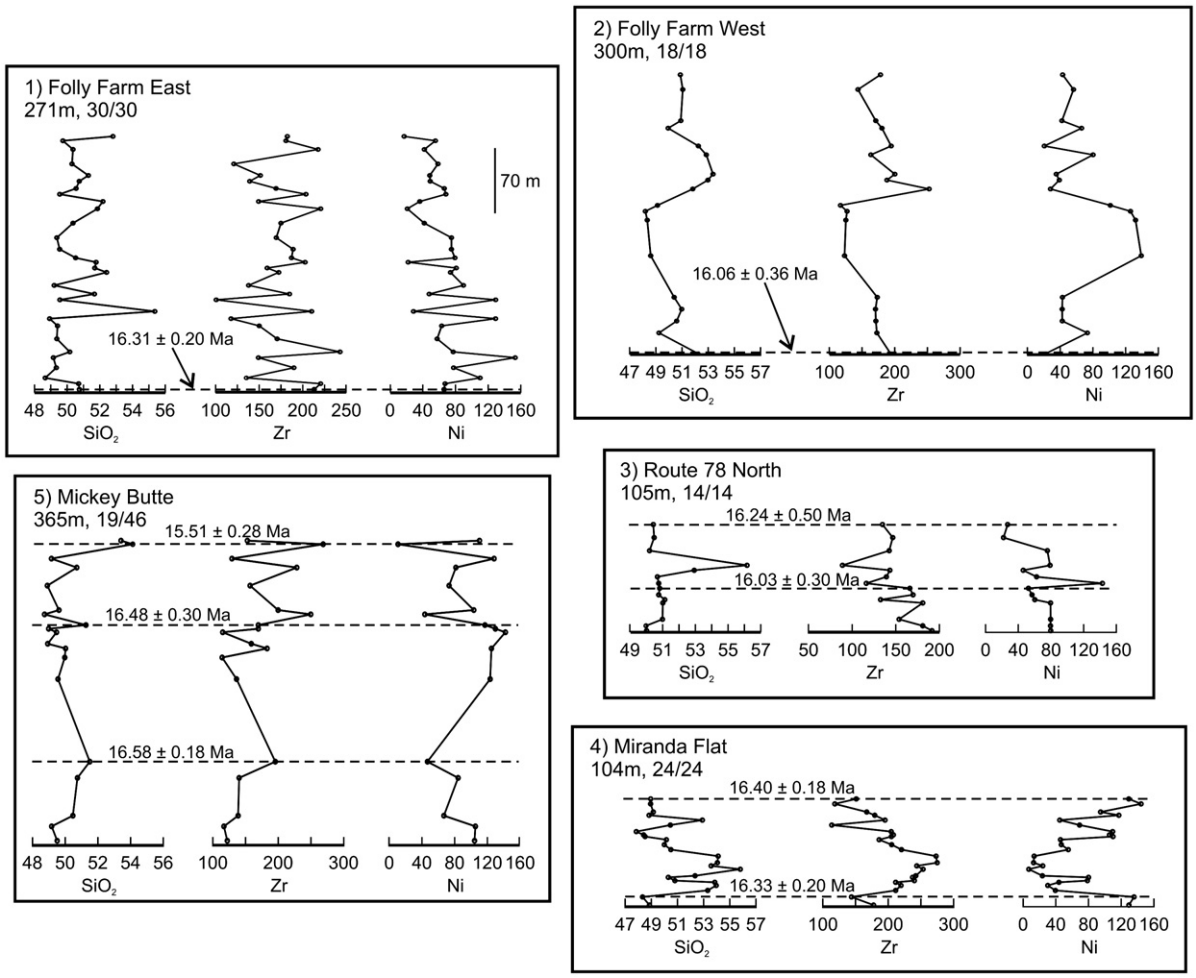

Fig. 10. Chemostratigraphic variation diagrams from sampled stratigraphic sections, discussed in this study. All five sections are depicted to scale and each point represents the stratigraphic position of sampled lava flows. Numbers below the section name are the thickness (m) and the number of sampled lava flows out of the total lava flows exposed. SiO_2 is expressed as weight percent oxide; Zr and Ni are expressed as ppm. The scale near the Folly Farm East section is applicable to all sections.

documented at their Steens Mountain type section (Gunn and Watkins, 1970; Carlson and Hart, 1983, 1987; Johnson et al., 1998) and from corresponding exposures to the south in the Pueblo Mountains (Hart et al., 1989). Oregon Plateau and Steens Basalt lava flows are dominantly basaltic, but also may be more chemically evolved, ranging in composition from ~48 to ~56 wt.% SiO_2 (Fig. 7a, b; Table 4; Appendix B; Chemistry). Additionally, Steens Basalt lava flows are tholeiitic to mildly alkaline, unlike other mid-Miocene and younger mafic calc-alkaline units that are exposed regionally and primarily associated with localized graben-forming events (Cummings et al., 2000; Hooper et al., 2002; Camp et al., 2003). Fig. 8a, b illustrate the relative iron enrichment of Steens lava flows from the type section as well as those Oregon Plateau flood basalts reported in this study. Two lava flows from this study plot as transitional to calc-alkaline. However, like those from the type section, the remainder of the samples are clearly tholeiitic. The two samples that are mildly calc-alkaline also have 53–57 wt.% SiO_2 and $K/P > 10$ suggesting that their calc-alkaline nature may be a function of interaction with Fe-poor material coupled with fractional crystallization. A role for AFC processes has previously been suggested to account for some of the observed Oregon Plateau flood basalt geochemical variability (Carlson and Hart, 1987; Hart et al., 1989).

Camp et al. (2003) used lower TiO_2/P_2O_5 ratios and other chemical criteria (e.g. lower average Sr and Ba values) to differentiate Steens Basalt lava flows from a group of chemically similar mid-Miocene tholeiitic lava flows they called Venator Ranch basalts. These Venator

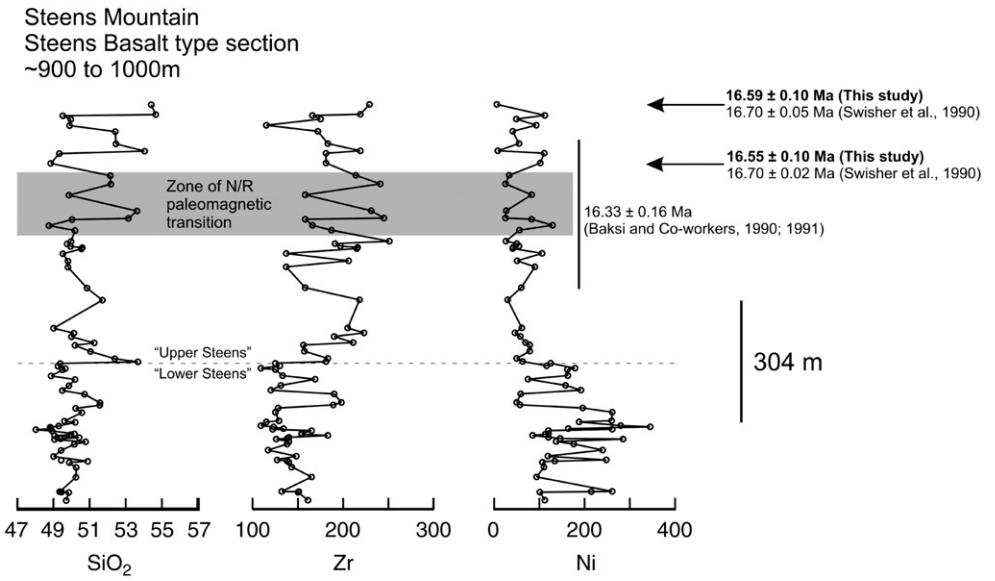

Fig. 11. Chemostratigraphic variation of the Steens Basalt at Steens Mountain (data from Johnson et al., 1998 hung at approximate stratigraphic position to depict within section chemical variation and is shown to illustrate the broad chemical variation within the section). $^{40}Ar/^{39}Ar$ ages from Baksi and Farrar (1990), Baksi et al. (1991), and Swisher et al. (1990) are also shown at their approximate stratigraphic positions and normalized to a 28.02 Ma age for the Fish Canyon tuff standard. Also, the approximate stratigraphic "zone" that the N/R polarity change present at this location is found within is depicted in gray (based on the detailed stratigraphy of Mankinen et al., 1985). "Upper" and "lower" Steens Basalt division of Binger (1997), Johnson et al. (1998) and Camp et al. (2003) is also depicted.

Ranch lava flows are primarily exposed to the north and west of the study area, but a few lava flows with Venator Ranch chemical signatures appear to be interbedded with Steens Basalt near the top of the Steens package at Steens Mountain (Camp et al., 2003). Fig. 9a, b illustrates the TiO_2/P_2O_5 variation of Oregon Plateau lava flows from this study and Steens Basalt lava flows from Steens Mountain, as well as the other tholeiites discussed by Camp et al. (2003). It is apparent that most of the lava flows sampled in this study have TiO_2/P_2O_5 values similar to the Steens Basalt lava flows from Steens Mountain and lie along the same general trend of increasing TiO_2 and P_2O_5. Also noticeable is that a number of samples from the Miranda Flat section have P_2O_5 values more similar to or higher than Venator Ranch lava flows. However, these lava flows have higher average Sr (623 to 730 ppm) and Ba (753 to 1023 ppm) values than Venator Ranch lava flows (Camp et al., 2003; Fig. 8a). These Venator Ranch-like samples are only found at the Miranda Flat section, where they are primarily exposed in its lower portion as two packages of three to four lava flows. These may either reflect the presence of a localized magmatic system or regionally derived lava flows that flowed to Miranda Flat.

At a regional level, major and trace element concentrations of Steens Basalt are consistent with their derivation via fractional crystallization of more primitive magmas, coupled with open-system processes (e.g. crustal assimilation; Carlson and Hart, 1987; Hart et al., 1989). Hart et al. (1989) studied ~17 to ~16 Ma flood basalts exposed in the Pueblo Mountains (the southern continuation of Steens Mountain) and demonstrated that the same isotopic and geochemical variations found at the Steens Basalt type section are found in an ~1 km section of flood basalt lava flows to the south and can be attributed to assimilation-fractional crystallization (AFC) processes. These identical variations (increasing incompatible element abundance and more radiogenic $^{87}Sr/^{86}Sr$ isotope ratios that correspond to increased stratigraphic level) demonstrate that Steens Basalt crops out to the south, at least to the Nevada border. Similar up-section chemical variations led Binger (1997), Johnson et al. (1998), and Camp et al. (2003) to divide the Steens Basalt at Steens Mountain into "upper" and "lower" Steens Basalt. While up section chemical and isotopic variations are virtually identical between the Steens Basalt at Steens Mountain and the Steens lava flows in the Pueblo Mountains, the presence of abundant dikes in close association with the Pueblo flood basalts suggests that some of the exposed lava flows in this region were erupted locally (Hart et al., 1989). Recent paleomagnetic work (Jarboe et al., 2003) reveals a N/R polarity reversal in the Pueblo Mountain

section, supporting the chemical and age data of Hart et al. (1989) that links this package of Steens Basalt to the lava flows exposed at Steens Mountain.

In the following discussion we present data that verifies the chemical correlation between Steens Basalt and the ~16±1 Ma basalts from this study. For clarity, these regional ~16±1 Ma flood basalts will be termed Oregon Plateau flood basalts throughout the remainder of this section. Additionally, for geochemical comparison, we have also divided Steens Basalt lava flows from the type section into the "upper" and "lower" Steens Basalt of previous workers (e.g. Binger, 1997; Johnson et al., 1998; Camp et al., 2003). Without discussing each section in detail, Figs. 10 and 11 illustrate the broad chemical variation of Oregon Plateau flood basalts and the Steens Basalt exposed at Steens Mountain. It is clear that within-section chemical variability of Oregon Plateau flood basalts is common at all locations (Fig. 10). In addition, while less evolved compositions are present within the lower ~400 m of lava flows exposed at Steens Mountain (Fig. 11; e.g. higher Ni, lower Zr and other incompatible trace element concentrations, lower average SiO_2), chemically similar lavas flows are occasionally exposed in the upper portion of the section. Additionally, similar, less evolved lava flows are exposed at all of the newly sampled locations (Fig. 10). Between section correlations of individual lava flows and flow packages from this study and Steens Basalt from Steens Mountain based on petrographic and bulk chemical characteristics were attempted through a number of statistical means, but in all cases, proved unsuccessful (Brueseke and Hart, 1999). We believe that this is not due to the inherent geochemical heterogeneity within individual lava flows, but rather is a direct result of the volcanic systems that were active in this region. For example, at the Mickey Butte location, the substantial age difference near the top of the section corresponds with significant major and trace element chemical differences (Fig. 10). These variations at Mickey Butte and the other investigated locations, likely reflect the presence of multiple, localized eruptive systems.

While correlation of lava flows and flow packages between the stratigraphic sections reported in this study proved unsuccessful, the gross chemical characteristics of these Oregon Plateau flood basalts allow them to be placed into a regional stratigraphic context. At Steens Mountain, "lower" Steens Basalt chemical signatures dominate the lower one-third of the section, while "upper" Steens Basalt chemical signatures occur primarily in the remaining two-thirds (Camp et al., 2003). K_2O and Ba concentrations have been utilized as good discriminators of "upper" and "lower" Steens Basalt chemical signatures in previous work at the Steens type section (e.g. Camp et al., 2003; Vic Camp, personal communication). There, the lava flows identified as "upper Steens" have Ba concentrations greater than 300 ppm and K_2O concentrations typically greater than 1 wt.%. Fig. 12 illustrates the TiO_2/P_2O_5, K_2O, and Ba values for the Oregon Plateau flood basalts from this study and the Steens Basalt from Steens Mountain. On these diagrams, it is apparent that the majority of samples from this study have wt.% $K_2O>1$ and $Ba>300$ ppm, most similar to the "upper Steens" Basalt. Only 12 Oregon Plateau flood basalts have Ba concentrations <300 ppm, like the "lower" Steens Basalt. These observations suggest that the majority of the Oregon Plateau lava flows from this study should be

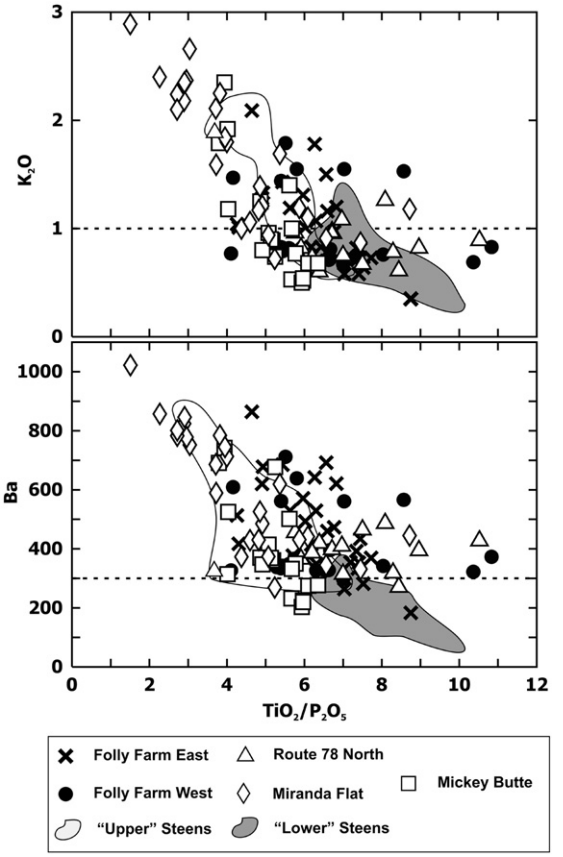

Fig. 12. (a) Plot of TiO_2/P_2O_5 vs. K_2O (wt.%) comparing the compositional variation of Oregon Plateau flood basalts from this study and Steens Basalt lava flows from Steens Mountain (Johnson et al., 1998). It is apparent that many of the newly sampled lava flows have K_2O values >1 wt.%, similar to the "upper" Steens Basalt. Dashed line drawn at 1 wt.% K_2O. (b) Plot of TiO_2/P_2O_5 vs. Ba (ppm) comparing the compositional variation of Oregon Plateau flood basalts from this study and Steens Basalt lava flows from Steens Mountain (Johnson et al., 1998). It is apparent that most of the newly sampled lava flows have Ba >300 ppm, similar to the "upper" Steens Basalt. Dashed line drawn at 300 ppm Ba.

considered "upper" Steens Basalt based on their chemical characteristics. Similar within section variations of interbedded "lower" and "upper" Steens lava flows are also noted by Binger (1997) and Camp et al. (2003), at the northern edge of the Oregon Plateau and are present in the Steens type section where the transition between "upper" and "lower" Steens Basalt is present (Johnson et al., 1998). The chronologic relationships between the Oregon Plateau flood basalts from this study and the Steens type section substantiate these chemical similarities and indicate that the lava flows in this study should be considered as Steens Basalt sensu-stricto.

5. Regional implications and significance

To reiterate, the nine new $^{40}Ar/^{39}Ar$ ages obtained on Steens Basalt lava flows range from 15.51±0.28 Ma to 16.58±0.18 Ma and the two lava flows originally dated by Swisher et al. (1990) from the type Steens section yield new, essentially identical ages of 16.59±0.10 Ma (uppermost) and 16.55±0.10 Ma (31st down). Conservatively, these data define a 1.05±0.46 m.y. duration of local (to Steens Mountain) Steens flood basalt volcanism. This age range does not take into consideration the 15.17±0.36 Ma age of the upper Folly Farm West tholeiitic andesite. Also, as previously mentioned, two of the youngest ages used in this calculation (MB97-40, 15.51±0.28 Ma; MB97-24, 16.06±0.36 Ma) are from samples that appear to have experienced argon loss and may only represent minimum eruption ages. However, the chemical and field evidence present at Mickey Butte (MB97-40 sampling location) that indicates the presence of an unconformity between MB97-40 and the underlying lava flows, lends credence to the validity of this younger age (Figs. 6 and 9, and unpublished data). As evident in Table 3, the time period over which much of the tholeiitic Malheur Gorge-region basalt was produced in east-central Oregon (Lees, 1994; Hooper et al., 2002) overlaps with Steens Basalt volcanism. Other age data that are included in this table are from older and possibly less precise K–Ar age determinations, as well as more recent $^{40}Ar/^{39}Ar$ data from chemically similar mafic lava flows present in the Owyhee Mountains and Santa Rosa–Calico volcanic field of northern Nevada (Shoemaker and Hart, 2003; Brueseke et al., 2003; Brueseke and Hart, in press).

Lees (1994) completed a study linking the flood basalts of the Malheur Gorge-region with the Imnaha and Grande Ronde basalts of the CRBG and connected the plagioclase-phyric and aphyric "lithotypes" found within the Malheur Gorge-region basalts to the dominantly plagioclase-phyric Imnaha and dominantly aphyric Grande Ronde Basalts. During this study it was suggested that these differing "lithotypes" might be the eruptive products of different stages of magma chamber development in multiple eruptive systems located throughout the Malheur Gorge-region over the duration of local flood basalt activity. This observation is very similar to what we observe in the vicinity of Steens Mountain, where multiple lithotypes of Steens Basalt crop out in stratigraphic sections independent of eruptive age. Following Lees (1994), Binger (1997) and Hooper et al. (2002) documented the geochemical and petrographic similarities between the Imnaha and Grand Ronde basalts, the Malheur Gorge-region basalts, and the "lower" and "upper" Steens Basalt exposed at Steens Mountain. Binger (1997) also noted that while the "upper" Steens Basalt is chemically evolved like the Birch Creek/Hunter Creek Basalts (Malheur Gorge-region) and the Grande Ronde Basalt, it is a chemically dissimilar unit. Furthermore, Camp et al. (2003)

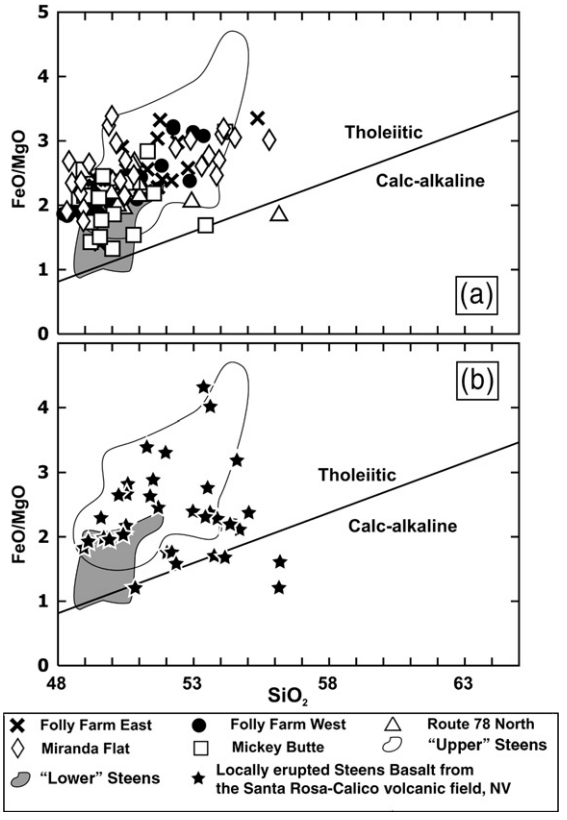

Fig. 13. (a) FeO/MgO vs. silica diagram of Miyashiro (1974) illustrating the tholeiitic vs. calc-alkaline affinities of Steens Basalt lava flows from Steens Mountain and Oregon Plateau flood basalts presented in this study. (b) Same diagram with only illustrating the tholeiitic vs. calc-alkaline affinities of locally erupted Steens Basalt from the Santa Rosa–Calico volcanic field, NV (unit Tba of Brueseke and Hart, in press).

suggested that the areal/volumetric extent of "upper" Steens Basalt decreases to the north of Steens Mountain, while lava flows with the "lower" Steens Basalt chemical affinity continue northward and physically link with the Lower Pole Creek lava flows of the Malheur Gorge-region. $^{40}Ar/^{39}Ar$ ages from these Malheur Gorge-region lava flows (Table 3; Lees, 1994; Hooper et al., 2002) are temporally indistinguishable and span a wide age-range. To better constrain their eruptive history and refine their age ranges, Hooper et al. (2002) calculated weighted mean ages for these Malheur–Gorge area units. Their calculations yield results of 16.9±0.8 Ma for two Lower Pole Creek flows ("lower" Steens Basalt equivalent), 16.5±0.3 Ma for four overlying Upper Pole Creek flows (Imnaha Basalt equivalent), and 15.7±0.1 Ma for three Birch Creek flows (Grande Ronde Basalt equivalent), all of which overlap with the chronostratigraphic results presented in this study.

Recent work has been performed by Brueseke and Hart (in press) to better understand the relationship between mid-Miocene mafic volcanism and the formation of large, silicic dominated volcanic fields on the Oregon Plateau (i.e. the early Snake River plain–Yellowstone volcanic fields). Included in this study are chemical and chronologic results from mafic lava flows and shallow intrusive bodies exposed along the southern Oregon Plateau/northern Nevada rift transition (i.e. the Santa Rosa–Calico volcanic field). Mafic Santa Rosa–Calico volcanic field (SC) extrusive and intrusive bodies are dominantly tholeiitic (Brueseke and Hart, in press) and are divided into two units that show interbedded relationships: (1) lava flows that are physically and chemically similar to the late-Miocene to Recent HAOT (high-alumina olivine tholeiite; Hart et al., 1984) basalts that crop out across the Oregon Plateau and (2) more evolved lava flows and shallow intrusive bodies that chemically resemble Steens Basalt (Brueseke and Hart, in press). The more evolved Steens-like unit is also the most areally extensive and voluminous of the two local mafic units. Fig. 13 illustrates the similarity between this SC unit (unit Tba of Brueseke and Hart, in press) and

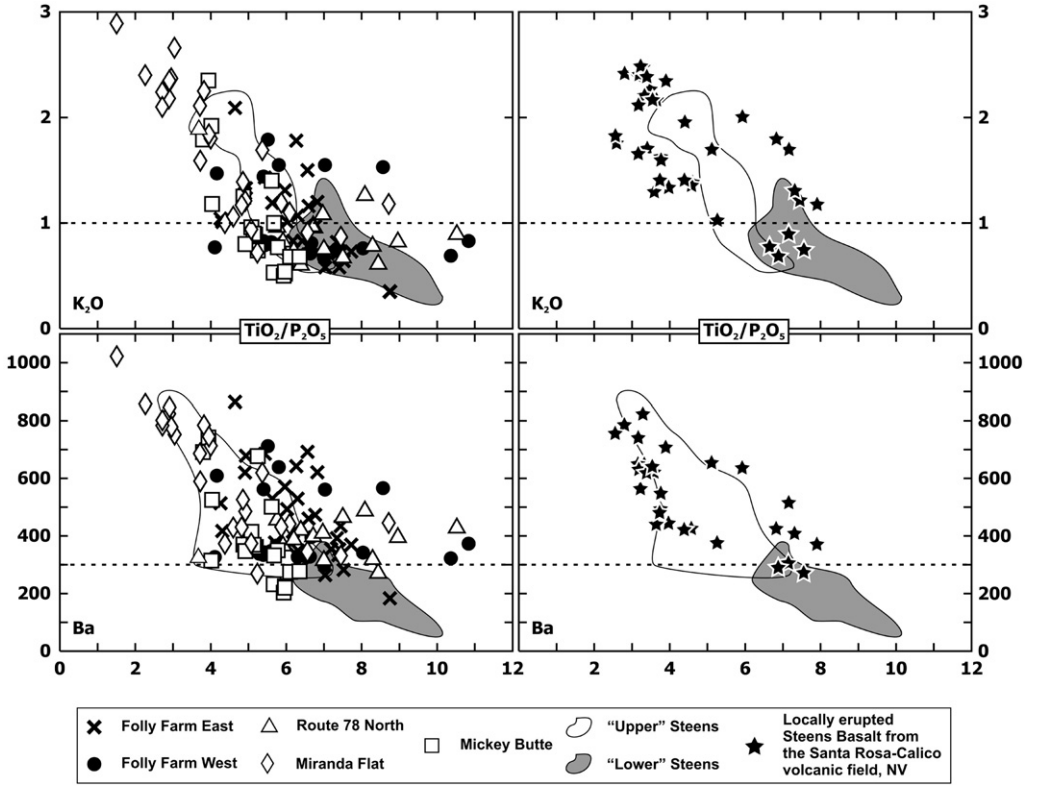

Fig. 14. Plot of TiO_2/P_2O_5 vs. K_2O (wt.%) and Ba (ppm) comparing the compositional variation of Oregon Plateau flood basalts from this study with Steens Basalt lava flows from Steens Mountain and the Santa Rosa–Calico volcanic field. It is apparent that many of the locally erupted Steens Basalt from the Santa Rosa–Calico volcanic field have K_2O values >1 wt.% and Ba >300 ppm, similar to the "upper" Steens Basalt and the lava flows reported in this study.

Steens Basalt lava flows from the type section and those from this study. The transitional to mildly calc-alkaline SC samples on Fig. 13b show extensive petrographic and chemical evidence indicating that they were affected by pre-eruptive open-system processes (e.g. assimilation of Fe-poor local crust and/or interaction with silicic melts), which can account for their low Fe and higher K concentrations and mildly calc-alkaline nature (Brueseke and Hart, in press; Brueseke, unpublished data). Fig. 14 illustrates the TiO_2/P_2O_5, wt.% K_2O, and Ba (ppm) values for these SC samples, Steens Basalt lava flows from the type section, and those from this study. It is apparent that SC mafic lava flows and shallow intrusive bodies have similar TiO_2/P_2O_5 values as the Steens Basalt. Also apparent is that the majority of these samples could be considered "upper" Steens Basalt based solely on geochemical criteria. The chemical similarities illustrated on Figs. 13 and 14 in addition to other petrographic, geochemical, and isotopic characteristics support the identification of these SC samples as locally erupted/emplaced Steens Basalt (Brueseke and Hart, in press). New $^{40}Ar/^{39}Ar$ ages obtained on representative samples from this Santa Rosa–Calico volcanic field mafic unit document that eruptions and upper-crustal emplacement of Steens Basalt magmas occurred locally from 16.73±0.04 to 14.35±0.38 Ma (standardized to 28.02 Ma Fish Canyon tuff) (Table 3; Brueseke and Hart, in press). These ages represent a much greater age range (~2.4 Ma) than those reported for the stratigraphic sections from this study and indicate that in the Santa Rosa–Calico volcanic field, lithospheric input (±eruption) of Steens Basalt magmas occurred over a longer duration than at both Steens Mountain and the other Oregon Plateau locations discussed in this study.

The observations discussed above indicate that mid-Miocene tholeiitic basaltic volcanism occurred over an ~2 m.y. duration at certain locations across the Oregon Plateau (e.g. the Santa Rosa–Calico volcanic field). This does not imply that widespread and voluminous flood basalt volcanism occurred continuously across the Oregon Plateau during the entire ~17 to ~14 Ma time period that the main phase of CRBG volcanism occurred. Rather it indicates that tholeiitic magmas with chemical characteristics identical to the Steens Basalt were emplaced into the Oregon Plateau lithosphere and occasionally erupted throughout this period. Additional work is required to more fully understand the areal extent, volume, and age of Steens Basalt exposed to the southwest and east/southeast of Steens Mountain. The time-transgressive nature of Steens volcanism indicates that the N/R magnetic reversal present within the upper portion of the Steens Mountain section may not be the only reversal present in regionally exposed packages of Steens Basalt. In summary, the field, chemical, and geochronologic data presented in this study convincingly reveal that Oregon Plateau flood basalt volcanism (e.g. Steens Basalt) is more complex and temporally extensive than often recognized.

6. Discussion and conclusions

New field observations, chemical analyses, and $^{40}Ar/^{39}Ar$ ages help to better document the duration of mid-Miocene Oregon Plateau basalt volcanism. These data and recent regional chronologic studies suggest that the main episode of Steens Basalt volcanism occurred for an ~1.05±0.46 m.y. duration and that in specific locations across the Oregon Plateau, less voluminous Steens volcanism occurred locally for a greater duration. Steens Basalt volcanism was intimately linked to both regional and local tectonomagmatic processes. Regionally, the Oregon Plateau has experienced greater extension in the last 20 Ma than the Columbia Plateau and likely experienced more widespread, but focused (at specific locations like the northern Nevada rift) extensional tectonism during the period of flood basalt volcanism (Carlson and Hart, 1987; Wells and Heller, 1988; Hooper and Conrey, 1989; Zoback et al., 1994; Cummings et al., 2000; Brueseke and Hart, in press). This extension also controlled the availability of upwelling Steens Basalt magma and led to the widespread areal distribution of Steens Basalt eruptive loci across the southeastern Oregon Plateau. During the mid-Miocene flood basalt event, the reactivation of regional lithospheric structural heterogeneities throughout the Oregon Plateau likely helped focus the upwelling mafic magma at locations that were actively extending and also helped localize the distribution of compositionally diverse (basalt through rhyolite) volcanism present at some of these locations (John and Wallace, 2000; Brueseke and Hart, 2004; Brueseke and Hart, in press; Brueseke et al., in press). For example, beneath the Santa Rosa–Calico volcanic field (Fig. 1), the continuous input of Steens magmas into the lithosphere was one of the primary driving mechanisms for local intermediate and silicic magma production (Brueseke and Hart, in press; Brueseke et al., in press). Similar processes likely occurred at other mid-Miocene Oregon Plateau silicic volcanic fields and eruptive loci (e.g. the McDermitt volcanic field).

While the upper portion of the type section at Steens Mountain only exposes ~16.6 Ma Steens Basalt lava flows, this flood basalt episode was more widespread temporally and geographically. Throughout the southern

Oregon Plateau, eruptive loci of mafic units interpreted to be Steens Basalt are found in the Owyhee Mountains (ID/OR), at Catlow Peak (OR), at Orevada View (OR), and near the Jordan Craters (OR) volcanic field (Mankinen et al., 1987; Hart, unpublished data). These mafic units are poorly constrained chemically and chronologically, so placing them into the "upper" and "lower" Steens Basalt stratigraphic nomenclature requires further work. In addition, ~17 to ~14 Ma mafic lava flows and dikes are found further south within the northern Nevada rift and its transition with the Oregon Plateau (Zoback et al., 1994; John and Wallace, 2000; Brueseke and Hart, in press), to the west in California (e.g. the ~16 Ma Lovejoy Basalt; Wagner et al., 2000; Coe et al., 2005), and ~16.5 Ma mafic lava flows are present to the east in the vicinity of the Jarbidge Mountains, ID (e.g. the Seventy-Six Basalt; Hart and Carlson, 1985; Rahl et al., 2002). The widespread locations of the other eruptive loci besides Steens Mountain proper (Fig. 1b), the lack of correlation between Steens Basalt sections on a flow-by-flow basis, and the presence of multiple flow units within Steens Basalt stratigraphic sections, reveal that during the span of Steens Basalt volcanism, numerous eruptive centers were active across the Oregon Plateau region. Recent work by Bondre et al. (2004) and Bondre and Hart (2006; personal communication) on the physical diversity of Steens Basalt lava flows at and in close proximity to Steens Mountain verifies this association at least locally and suggests that these lava flows erupted from onlapping and superimposed monogenetic volcanic systems. Based on these physical observations, Bondre and Hart (2006; personal communication) classify the Steens Basalt as a moderate-sized flood basalt field using the terminology of Walker (1993). Their physical evidence agrees with the chemical evidence presented in this study and illustrates a scenario where much of the Steens Basalt exposed in the vicinity of Steens Mountain may have been erupted via the plains-style basaltic volcanism of Greely (1982), similar to what is found across the present day Snake River Plain, Owyhee Plateau, and Oregon High Lava Plains, only at a larger scale. These observations do not preclude the presence of a large shield volcano centered at Steens Mountain as suggested by previous workers; they just indicate that magma evolution and eruptive processes in the vicinity of Steens Mountain were more complex than previously recognized. They also suggest that the eruptive style(s) of mid-Miocene Oregon Plateau flood basalt volcanism differed from the much more voluminous outpourings that characterized CRBG volcanism and lava flow emplacement. In essence, throughout the ~1.05±0.46 m.y. duration of local (to Steens Mountain) Steens volcanism, lava flows and flow units with chemical and petrographic variations similar to those exposed at Steens Mountain were sourced from numerous, scattered eruptive loci. During this period, any lithologic type of Steens Basalt was erupted at any given vent and likely related to local magma chamber processes. The chemical composition of lava flows during this period was dominated by "upper" Steens compositions regardless of lithologic type and the results of this study help define their apparent position in the regional Pacific Northwest flood basalt stratigraphic record compiled by other workers (Hooper et al., in press).

While the most volumetric tholeiitic volcanism in the Pacific Northwest may have been present to the north, contemporaneous lithospheric input (±eruption) of basaltic magmas was occurring on the southern Oregon Plateau over a longer duration than what is represented at Steens Mountain. The field observations, chemical data, and $^{40}Ar/^{39}Ar$ geochronology presented in this study agree with this prior observation and accordingly, provide a more precise temporal link between eruptions of the Steens Basalt and other regionally extensive flood basalts. This refined temporal link requires that petrogenetic and tectonic models of mid-Miocene northwestern U.S. flood basalt volcanism recognize that the northern (Columbia Plateau) and southern (Oregon Plateau) portions of this flood basalt province were erupting simultaneously at times other than just at the onset of regional activity. This does not imply that Oregon Plateau flood basalt volcanism continued without cessation throughout the larger flood basalt event or was coeval with the entire CRBG. However, the intimate link between the timing of mid-Miocene Oregon Plateau silicic and intermediate volcanic field development (e.g. McDermitt, Lake Owyhee, Northwest Nevada, and Santa Rosa–Calico) and Steens Basalt volcanism implies a petrogenetic connection between basalt production and the development of regional polygenetic volcanic fields and caldera complexes. The availability of upwelling mafic magma into the lithosphere affected the duration and location of the coeval intermediate through silicic volcanism in these systems. In summary, these data indicate that the same large-scale mantle processes controlling the generation and eruption of the CRBG on the Columbia River Plateau were similarly affecting the Oregon Plateau throughout the mid-Miocene, not just at ~16.7 Ma, when widespread Oregon Plateau basaltic volcanism likely initiated. As a result, tectonomagmatic models (e.g. mantle plume, non-plume, or others) that are invoked to explain this regional flood basalt event must

consider the full duration of flood basalt volcanism and mafic magma lithospheric input on the Oregon Plateau.

Acknowledgements

We thank John Morton (Miami University) for his assistance with DCP-AES elemental analyses and Claire McKee for her assistance in the field. Vic Camp and Peter Hooper provided thorough reviews of previous versions of this manuscript and we thank Bruce Marsh for his editorial attention and help. We also thank Ed Mankinen (U.S.G.S.) for his help with answering specific questions about the magnetostratigraphic record present within the Steens Basalt at Steens Mountain and for helping to determine the precise stratigraphic locations of previously dated lava flows from the type Steens section. National Science Foundation Grant EAR-0106144 (Hart), a Miami University Faculty Research Grant (Hart), and a Geological Society of America Student Research Grant (Brueseke) have provided the necessary financial support for this research.

Appendix A. Supplementary data

Supplementary data associated with this article can be found, in the online version, at doi:10.1016/j.jvolgeores.2006.12.004.

References

Armstrong, R.L., Taubeneck, W.P., Hales, P.O., 1977. Rb–Sr and K–Ar geochronology of Mesozoic granitic rocks and their Sr isotopic compositions, Oregon, Washington, and Idaho. Geol. Soc. Amer. Bull. 88, 397–411.

Avent, J.C., 1970. Correlation of the Steens–Columbia River Basalts: some tectonic and petrogenetic implications. In: Gilmour, E.H., Stradling, D. (Eds.), Proceedings of the Second Columbia River Basalt Symposium. Cheney, Washington, pp. 133–156.

Baksi, A.K., 1999. Reevaluation of plate motion models on hotspot tracks in the Atlantic and Indian Oceans. J. Geol. 107, 13–26.

Baksi, A.K., Farrar, E., 1990. Evidence for errors in the geomagnetic polarity time-scale at 17–15 Ma: $^{40}Ar/^{39}Ar$ dating of basalts from the Pacific northwest, USA. Geophys. Res. Lett. 17, 1117–1120.

Baksi, A.K., Watkins, N.D., York, D., 1967. Age of the Steens Mountain geomagnetic polarity transition. J. Geophys. Res. 72, 6299–6308.

Baksi, A.K., Hall, C.H., York, D., 1991. Laser probe $^{40}Ar/^{39}Ar$ dating studies on sub-milligram whole-rock basalt samples: the age of the Steens Mountain geomagnetic polarity transition (revisited). Earth Planet. Sci. Lett. 104, 292–298.

Binger, G.B., 1997. The volcanic stratigraphy of the Juntura region, eastern Oregon. M.S. Thesis, Washington State University, Pullman, Washington, 140 pp.

Brueseke, M.E., Hart, W.K., 1999. Stratigraphy and whole rock chemistry of mid-Miocene lava flows in the vicinity of Steens Mountain, southeastern Oregon. Geol. Sci. Am. Abs. Prog. 31, 5.

Brueseke, M.E., Hart, W.K., 2002. Mid-Miocene flood basalt volcanism in southeastern Oregon: new insights on an old problem. Geol. Sci. Am. Abs. Prog. 34, 364.

Brueseke, M.E., Hart, W.K., 2004. The physical and petrologic evolution of a multi-vent volcanic field associated with Yellowstone–Newberry volcanism. Eos Trans. AGU 85, 47.

Brueseke, M.E., Hart, W.K. (in press). Geology and Petrology of the mid-Miocene Santa Rosa–Calico volcanic field, northern Nevada: Nevada Bureau of Mines and Geology Bulletin 112, xx p.

Brueseke, M.E., Hart, W.K., Wallace, A.R., Heizler, M.T., Fleck, R.J., 2003. Mid-Miocene volcanic field development in northern Nevada: new age constraints on the timing of Santa Rosa–Calico volcanism. Geol. Sci. Am. Abs. Prog. 35, 63.

Brueseke, M.E., Hart, W.K., Heizler, M.T. (in press). Chemical and physical diversity of mid-Miocene silicic volcanism in northern Nevada: Bull. Volc.

Bondre, N.R, Hart, W.K., 2006. Morphological and textural diversity of Steens Basalt lava flows, southeastern Oregon, USA: implications for emplacement style and nature of eruptive episodes. Eos Trans. AGU 87, 52.

Bondre, N.R., Duraiswami, R.A., Dole, G., 2004. A brief comparison of lava flows from the Deccan Volcanic Province and the Columbia–Oregon Plateau Flood Basalts: implications for models of flood basalt emplacement. Proc. Indian Acad. Sci. (Earth Planet. Sci.) 113, 809–817.

Camp, V.E., Ross, M.E., 2004. Mantle dynamics and genesis of mafic magmatism in the intermontane Pacific Northwest. J. Geophys. Res. 109, B08204. doi:10.1029/2003JB002838.

Camp, V.E., Ross, M.E., Hanson, W.E., 2003. Genesis of flood basalts and Basin and Range volcanic rocks from Steens Mountain to the Malheur River Gorge, Oregon. Geol. Soc. Amer. Bull. 115, 105–128.

Carlson, R.W., Hart, W.K., 1983. Geochemical study of the Steens Mountain flood basalt. Carnegie Inst. Wash. Yearbook 82, 475–481.

Carlson, R.W., Hart, W.K., 1987. Crustal genesis on the Oregon Plateau. J. Geophys. Res. 92, 6191–6206.

Christiansen, R.L., McKee, E.H., 1978. Late Cenozoic volcanic and tectonic evolution of the Great Basin and Columbia Intermontane region. In: Smith, R.B., Eaton, G.P. (Eds.), Cenozoic tectonics and regional geophysics of the western Cordillera. Geol. Soc. Am. Mem., vol. 152. Denver, Colorado, pp. 283–312.

Christiansen, R.L., Evans, J.R., Foulger, G.R., 2002. Upper-mantle origin of the Yellowstone Hotspot. Geol. Soc. Amer. Bull. 111, 1245–1256.

Coe, R.S., Stock, G.M., Lyons, J.L., Beitler, B., Bowen, G.J., 2005. Yellowstone hotspot volcanism in California? A paleomagnetic test of the Lovejoy flood basalt hypothesis. Geology 33, 697–700.

Colgan, J.P., Dumitru, T.A., McWilliams, M., Miller, E.L., 2006. Timing of Cenozoic volcanism and Basin and Range extension in northwestern Nevada: new constraints from the northern Pine Forest Range. Geol. Soc. Amer. Bull. 118, 126–139.

Crafford, E.E.J., Grauch, V.J.S., 2002. Geologic and geophysical evidence for the influence of deep crustal structures on Paleozoic tectonics and the alignment of world-class gold deposits, north-central Nevada, USA. Ore Geol. Rev. 21, 157–184.

Cummings, M.L., Evans, J.G., Ferns, M.L., Lees, K.R., 2000. Stratigraphic and structural evolution of the middle Miocene syn-volcanic Oregon–Idaho graben. Geol. Soc. Amer. Bull. 112, 668–682.

Deino, A., Potts, R., 1990. Single-Crystal $^{40}Ar/^{39}Ar$ dating of the Olorgesailie Formation, Southern Kenya Rift. J. Geophys. Res. 95, 8453–8470.

Dickinson, W.R., 1997. Overview: tectonic implications of Cenozoic volcanism in coastal California. Geol. Soc. Amer. Bull. 109, 936–954.

Fleck, R.J., Sutter, J.F., Elliot, D.H., 1977. Interpretation of discordant $^{40}Ar/^{39}Ar$ age-spectra of Mesozoic tholeiites from Antarctica. Geochim. Cosmochim. Acta 41, 15–32.

Fuller, R.E., 1930. The petrology and structural relationship of the Steens Mountain Volcanic Series of southeastern Oregon. Ph.D. dissertation, University of Washington, Seattle, 282.

Fuller, R.E., 1931. The geomorphology and volcanic sequence of Steens Mountain in southeastern Oregon. Wash. Univ. Pub. Geol. 3, 1–130.

Glen, J.M.G., Ponce, D.A., 2002. Large-scale fractures related to the inception of the Yellowstone hotspot. Geology 30, 647–650.

Greely, R., 1982. The Snake River Plain, Idaho: representative of a new category of volcanism. J. Geophys. Res. 87, 2705–2712.

Grommé, C.S., Mankinen, E.A., Prévot, M., Coe, R.S., 1985. Steens Mountain geomagnetic polarity transition is a single phenomenon. Nature 318, 487–488.

Gunn, B.M., Watkins, N.D., 1970. Geochemistry of the Steens Mountain Basalts, Oregon. Geol. Soc. Amer. Bull. 81, 1497–1516.

Hart, W.K., Mertzman, S.A., 1982. K–Ar ages of basalts from southcentral and southeastern Oregon. Isochron-West 33, 23–26.

Hart, W.K., Carlson, R.W., 1985. Distribution and geochronology of Steens Mountain-type basalts from the northwestern Great Basin. Isochron-West 43, 5–10.

Hart, W.K., Aronson, J.L., Mertzman, S.A., 1984. Areal distribution and age of low-K high alumina olivine tholeiite magmatism in the northwestern Great Basin. Geol. Soc. Amer. Bull. 95, 185–195.

Hart, W.K., Carlson, R.W., Mosher, S.A., 1989. Petrogenesis of the Pueblo Mountains basalt, southeastern Oregon and northern Nevada. In: Reidel, S.P., Hooper, P.R. (Eds.), Volcanism and tectonism in the Columbia River flood-basalt province. Geol. Soc. Am. Spec. Pap., vol. 239. Denver, Colorado, pp. 367–378.

Heizler, M.T., Perry, F.V., Crowe, B.M., Peters, L., Appelt, R., 1999. The age of Lathrop Wells Volcanic Center: an $^{40}Ar/^{39}Ar$ dating investigation. J. Geophys. Res. 104, 767–804.

Henry, C.D., Castor, S.B., McIntosh, W.C., Heizler, M.T., Cuney, M., Chemillac, R., 2006. Timing of oldest Steens Basalt magmatism from precise dating of silicic volcanic rocks, McDermitt caldera and northwest Nevada volcanic field. Eos Trans. AGU 87, 52.

Hook, R., 1981. The volcanic stratigraphy of the Mickey hot spring area, Harney County, Oregon. M.S. Thesis, Corvallis, Oregon, Oregon State University, 66 pp.

Hooper, P.R., 1997. The Columbia River Flood Basalt province: current status. In: Mahoney, J.J., Coffin, M.F. (Eds.), Large Igneous Provinces: continental, oceanic, and planetary flood volcanism. AGU Geophys. Mono. Ser., vol. 100, pp. 1–27. Washington D.C.

Hooper, P.R., 2000. Chemical discrimination of Columbia River basalt flows. Geochem. Geophys. Geosyst. 1, (Article), 2000GC000040 [5609 words], 2000.

Hooper, P.R., Conrey, R.M., 1989. A model for the tectonic setting of the Columbia River basalt eruptions. In: Reidel, S.P., Hooper, P.R. (Eds.), Volcanism and tectonism in the Columbia River flood-basalt province. . Geol. Soc. Am. Spec. Pap., vol. 239. Denver, Colorado, pp. 293–306.

Hooper, P.R., Binger, G.B., Lees, K.R., 2002. Age of the Steens and Columbia River flood basalts and their relationship to extension-related calc-alkalic volcanism in eastern Oregon. Geol. Soc. Amer. Bull. 114, 43–50.

Hooper, P.R., Camp, V.E., Reidel, S.P., Ross, M.E., (in press). Origin of the Columbia River Flood Basalts: Plume vs. Nonplume Models. In: Foulgar, G.R., Judy, D.M. (Eds.), The Origins of Melting Anomalies: Plates, Plumes, and Planetary Processes. Geol. Soc. Am. Spec. Pap.

Humphreys, E.D., Dueker, K.G., Schutt, D.L., Smith, R.B., 2000. Beneath Yellowstone: evaluating plume and nonpplume models using telesiesmic images of the upper mantle. GSA Today 10, 1–6.

Jarboe, N.A., Coe, R.S., Glen, J.M., Renne, P.R., 2003. A study of mid-Miocene Yellowstone hotspot volcanics and the search for the Steens Mountain reversal. Eos Trans. AGU 84, 46.

Jarboe, N.A., Coe, R.S., Renne, P.R., Glen, J.M., 2006. $^{40}Ar/^{39}Ar$ ages of the early Columbia River Basalt Group: determining the Steens Mountain Geomagnetic Polarity Reversal (R_0–N_0) as the top of the C5Cr Chron and the Imnaha Normal (N_0) as the C5Cn.3n Chron. Eos Trans. AGU 87, 52.

John, D.A., 2001. Miocene and early Pliocene epithermal gold–silver deposits in the northern Great Basin, western United States: characteristics, distribution, and relationship to magmatism. Econ. Geol. 96, 1827–1853.

John, D.A., Wallace, A.R., 2000. Epithermal gold–silver deposits related to the northern Nevada Rift: Geology and Ore Deposits 2000. The Great Basin and Beyond Symposium: Geol. Soc. Nev. Proc., pp. 155–175.

Johnson, J.A., 1995. Geologic evolution of the Duck Creek Butte eruptive center, High Lava Plains, southeastern Oregon. M.S. Thesis, Corvallis, Oregon, Oregon State University, 168 pp.

Johnson, J.A., Hawkesworth, C.J., Hooper, C.J., Binger, P.R., 1998. Major- and trace-element analyses of Steens Basalt, Southeastern Oregon. U.S. Geol. Surv. Open File Rep., vol. 98-482, p. 30.

Jordan, B.T., Grunder, A.L., Duncan, R.A., Deino, A.L., 2004. Geochronology of age-progressive volcanism of the Oregon High Lava Plains: implications for the plume interpretation of Yellowstone. J. Geophys. Res. 109, B10202. doi:10.1029/2003JB002776.

Katoh, S., Danhara, T., Hart, W.K., WoldeGabriel, G., 1999. Use of sodium polytungstate solution in the purification of volcanic glass shards for bulk chemical analysis. Nat. Hum. Act. 4, 45–54.

Kistler, R.W., Peterman, Z.E., 1978. Reconstruction of crustal California on the basis of initial strontium isotopic compositions of Mesozoic granitic rocks. U. S. Geol. Surv. Prof. Pap., vol. 107, pp. 1–17.

Lanphere, M.A., Baadsgaard, H., 2001. Precise K–Ar, $^{40}Ar/^{39}Ar$, Rb–Sr, and U/Pb mineral ages from the 27.5 Ma Fish Canyon tuff reference standard. Chem. Geol. 175, 653–671.

Larson, E.E., Watson, D.E., Jennings, W., 1971. Regional comparison of a Miocene geomagnetic transition in Oregon and Nevada. Earth Planet. Sci. Lett. 11, 391–400.

LeBas, M.J., Le Maitre, R.W., Streckeisen, A., Zanettin, B., 1986. A chemical classification of volcanic rocks based on the total alkali-silica diagram. J. Petrol. 27, 745–750.

Leeman, W.P., Oldow, J.S., Hart, W.K., 1992. Lithosphere-scale thrusting in the western U.S. Cordillera as constrained by Sr and Nd isotopic transitions in Neogene volcanic rocks. Geology 20, 63–66.

Lees, K.R., 1994. Magmatic and tectonic changes through time in the Neogene volcanic rocks of the Vale area, Oregon, North Western USA. Ph.D. dissertation, Milton Keynes, United Kingdom, The Open University, 284 pp.

Mahon, K.I., 1996. The New "York" regression: application of an improved statistical method to geochemistry. Int. Geol Rev. 38, 293–303.

Mankinen, E.A., Prévot, M., Grommé, C.S., Coe, R.S., 1985. The Steens Mountain (Oregon) geomagnetic polarity transition 1. Directional history, duration of episodes, and rock magmatism. J. Geophys. Res. 90, 10,393–10,416.

Mankinen, E.A., Larson, E.E., Grommé, C.S., Prévot, M., Coe, R.S., 1987. The Steens Mountain (Oregon) geomagnetic polarity transition 3. Its regional significance. J. Geophys. Res. 92, 8057–8076.

McDougall, I., Harrison, T.M., 1999. Geochronology and Thermochronology by the $^{40}Ar/^{39}Ar$ Method. Oxford University Press. 269 pp.

Mertzman, S.A., 2000. K–Ar results from the southern Oregon–northern California Cascade Range. Ore. Geol. 62, 99–122.

Miyashiro, A., 1974. Volcanic rock series in island arcs and active continental margins. Am. J. Sci. 274, 321–355.

Perkins, M.E., Nash, B.P., 2002. Explosive silicic volcanism of the Yellowstone Hotspot: the ash fall tuff record. Geol. Soc. Amer. Bull. 114, 367–381.

Rahl, J.M., Foland, K.A., McGrew, A.J., 2002. Transition from contraction to extension in the northeastern Basin and Range: new evidence from the Copper Mountains, Nevada. J. Geol. 110, 179–194.

Renne, P.R., Swisher, C.C., Deino, A.L., Karner, D.B., Owens, T.L., DePaolo, D.J., 1998. Intercalibration of standards, absolute ages and uncertainties in $^{40}Ar/^{39}Ar$ dating. Chem. Geol. 145, 117–152.

Rytuba, J.J., McKee, E.H., 1984. Peralkaline ash flow tuffs and calderas of the McDermitt volcanic field, southeast Oregon and north central Nevada. J. Geophys. Res. 89, 8616–8628.

Sherrod, D.R., Minor, S.A., Vercoutere, T.L., 1989. Geologic map of the Sheepshead Mountains, Harney and Malheur counties, Oregon. United States Geol. Surv. Misc. Field Stud. Map MF-2079, 1 sheet.

Shoemaker, K.A., Hart, W.K., 2003. Temporal controls on basalt genesis and evolution on the Owyhee plateau, Idaho and Oregon. In: Bonnichsen, B., White, C.M., McCurry, M. (Eds.), Tectonic and magmatic evolution of the Snake River Plain volcanic province. Idaho Geol. Surv. Bull., vol. 30. 16 pp.

Singer, B.S., Pringle, M.S., 1996. Age and duration of the Matuyama–Brunhes geomagnetic polarity reversal from $^{40}Ar/^{39}Ar$ incremental heating analyses of lavas. Earth Planet. Sci. Lett. 139, 47–61.

Smith, J.A., 1987. Volcanism and Paleomagnetism of the Sheepshead Mountains, Oregon. Undergraduate Thesis, Lancaster, Pennsylvania, Franklin and Marshall College, 23 pp.

Stewart, M.A., 1992. Petrogenesis of high alumina flood basalts, Steens Mountains, Oregon. M.S. Thesis, Bloomington, Indiana, Indiana University, 65 pp.

Swisher, C.C., Ach, J.A., Hart, W.K., 1990. Laser fusion $^{40}Ar/^{39}Ar$ dating of the type Steens Mountain Basalt, southeastern Oregon and the age of the Steens geomagnetic polarity transition. Eos Trans. AGU 71, 1296.

Tolan, T.L., Reidel, S.P., Beeson, M.H., Anderson, J.L., Fecht, K.R., Swanson, D.A., 1989. Revisions to the estimates of the areal extent and volume of the Columbia River Basalt Group. In: Reidel, S.P., Hooper, P.R. (Eds.), Volcanism and tectonism in the Columbia River flood-basalt province. . Geol. Soc. Am. Spec. Pap., vol. 239. Denver, Colorado, pp. 367–378.

Wagner, D.L., Deino, A.L., Renne, P.R., Saucedo, G.J., 2000. Age and origin of the Lovejoy Basalt of Northern California. Geol. Sci. Am. Abs. Prog. 32, 159.

Walker, G.P.L., 1993. Basaltic-volcano systems. In: Prichard, H.M., Alabaster, T., Harris, N.B.W., Neary, C.R. (Eds.), Magmatic Processes and Plate Tectonics. Geol. Soc. Spec. Pub., vol. 76, pp. 3–38. London.

Wells, R.E., Heller, P.L., 1988. The relative contribution of accretion, shear, and extension to Cenozoic tectonic rotation in the Pacific Northwest. Geol. Soc. Amer. Bull. 100, 325–338.

York, D., 1969. Least squares fitting of a straight line with correlated errors. Earth Planet. Sci. Lett. 5, 320–324.

Zoback, M.L., McKee, E.H., Blakely, R.J., Thompson, G.A., 1994. The northern Nevada rift: regional tectono-magmatic relations and middle Miocene stress direction. Geol. Soc. Amer. Bull. 106, 371–382.